

INNOVATIVE TECHNIQUE TO FABRICATE COST EFFECTIVE MICROBOLOMETER SENSOR USING FRONT END BULK MICROMACHINING

Chanda Karthik

A Dissertation Submitted to
Indian Institute of Technology Hyderabad
In Partial Fulfillment of the Requirements for
The Degree of Master of Technology



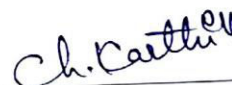
भारतीय प्रौद्योगिकी संस्थान हैदराबाद
Indian Institute of Technology Hyderabad

Department of Electrical Engineering

June, 2015

Declaration

I declare that this written submission represents my ideas in my own words, and where others' ideas or words have been included, I have adequately cited and referenced the original sources. I also declare that I have adhered to all principles of academic honesty and integrity and have not misrepresented or fabricated or falsified any idea/data/fact/source in my submission. I understand that any violation of the above will be a cause for disciplinary action by the Institute and can also evoke penal action from the sources that have thus not been properly cited, or from whom proper permission has not been taken when needed.



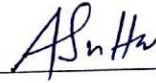
(Signature)

Chanda Karthik

EE13M1011

Approval Certificate

This Thesis entitled **Innovative Technique to Fabricate Cost Effective Microbolometer Sensor using Front End Bulk Micromachining** by **Mr. Chanda Karthik (EE13M1011)** is approved for the degree of **Master of Technology** from **IIT Hyderabad**.



Dr Asudeb Dutta

Assistant Professor, Dept. of EE, IITH
(Internal Examiner)



Dr. Sobhan Babu

Assistant Professor, Dept. of CSE, IITH
(External Examiner)



Dr. Shiv Govind Singh

Associate Professor, Dept. of EE, IITH
(Advisor)



Dr. Siva Rama Krishna Vanjari

Assistant Professor, Dept. of EE, IITH
(Chairman)

Acknowledgements

First and foremost I want to acknowledge and thank Dr. Shiv Govind Singh and Dr. Siva Rama Krishna Vanjari for their consistent guidance, support and help. Their constant motivation helped me to actively work for the project.

I want to thank Dr. Asudeb Dutta for helping me with his research experience.

I want to thank my family members and all my friends those helped me in completing my project successfully.

I am thankful to Radharamana Mohanty for his support in this project.

Dedicated to

My Family and friends.....

Abstract

Frontend bulk micro machining is one of the proven techniques of making suspended microstructures and is highly adapted due to its simple and cost effective way of fabricating the devices. We propose a novel geometric mask designs for achieving area efficient microstructures by frontend Si bulk micromachining.

In this work we adapt the geometric mask design having a microstructure between two rectangular openings. These openings are aligned at 45° to wafer prime flat of (100) silicon wafer and act as etch openings for frontend bulk micromachining. However rectangular openings lead to high silicon area consumption which makes the process unworthy. Therefore we proposed different geometries to minimize area consumption for achieving the same dimension of suspended structure. All these different geometries are simulated using Intellisuite FABSIM based physical simulator. We have observed more than 28% reduction in foot print over literature reported design.

Here, development of low-cost un-cooled infrared microbolometer detector is reported, where the Si itself is used as the infrared sensitive material. The process does not require any diffusion or electrochemical etch-stop technique unlike traditional CMOS line microbolometer fabrication. Rather we are reporting two ways of fabricating the device. The first method is done by using only one mask with only front end bulk micro machining using anisotropic and isotropic wet etchants. The second uses both DRIE and wet etching. The first method reduces the fabrication cost of the device drastically and the second method reduces the area per pixel.

Contents

Declaration.....	ii
Approval Sheet	iii
Acknowledgements.....	iv
Abstract.....	vi
Chapter 1 Introduction	1
1.1 Infrared and Infrared Detection.....	3
1.2 Motivation.....	3
1.3 Aim and Objective of Thesis.....	5
1.4 Thesis Outline.....	5
Chapter 2 Literature Survey	7
2.1 Fabrication of Si Microbriges and Cantilevers	7
2.2 Microbolometer and Fabrication	8
Chapter 3 Silicon Bulk Micromachining	11
3.1 Frontend Bulk micromachining to Make Si microbridges.....	11
3.2 Process flow to obtain Si Microbridge.....	13
3.3 Result and Discussion.....	15
Chapter 4 Simulation and Fabrication of Si Microbridges.....	18
4.1 Proposed Method to reduce area consumption for making Si Microbridges.....	18
4.2 Simulation and Fabrication of Area efficient Si microbridges.....	19
4.3 Comparative case study of the all area efficient mask Designs.....	22
Chapter 5 Microbolometer and design.....	23
5.1 Innovative methods for Fabricating Microbolometer.....	23
5.2 Process Simulation showing Microbolometer Fabrication using only Front end Bulk micromaching	24

5.2.1	Only using wet etching.....	24
5.2.1.1	Simulation Results.....	25
5.2.2	Dry etching followed by Wet etching.....	26
5.2.2.1	DRIE followed by TMAH etching.....	26
5.2.2.1.1	Simulation Results.....	28
5.2.2.2	DRIE followed by HNA etching.....	28
5.2.2.2.1	Simulation Results.....	29
Chapter 6	Efficient Method to Fabricate Microbolometer.....	30
6.1	Design and Simulation of area efficient Microbolometers	30
6.1.1	Only using wet etching.....	31
6.1.2	Dry etching followed by Wet etching.....	34
6.1.2.1	DRIE followed by TMAH etching.....	34
6.1.2.2	DRIE followed by HNA etching.....	37
Chapter 7	Fabrication results of Microbolometer.....	40
7.1	Microbolometer.....	40
7.2	Issues faced in fabrication process.....	42
7.2.1	Issue with negative photoresist.....	42
7.2.2	Side wall protection.....	44
7.3	HNA etching.....	45
7.4	Fabrication of array of microbolometers.....	50
Chapter 8	Comparative Case study of Making Microbolometer Sensor.....	52
8.1	Comparisons between only wet etching and dry followed by wet etching.....	52
8.2	Comparisons between sub methods under method-2.....	53
8.3	Comparisons between proposed methods and existing methods of making microbolometer sensor.....	54

Chapter 9 Conclusion and Future Work	55
9.1 Conclusion.....	55
9.2 Future Scope of Work.....	55
References	56

Chapter 1

Introduction

1.1 Infrared and Infrared Detection

Infrared (IR) is electromagnetic radiation with longer wavelengths than those of visible light, extending from the nominal red edge of the visible spectrum at 700 nanometers (nm) to 1 mm. Infrared radiation was discovered in 1800 by astronomer William Herschel, who discovered a type of invisible radiation in the spectrum beyond red light, by means of its effect upon a thermometer. Most of the thermal radiation emitted by objects near room temperature is infrared. Infrared radiation can be used to remotely determine the temperature of objects (if the emissivity is known), this is termed thermography.

Thermographic cameras detect radiation in the infrared range of the electromagnetic spectrum (roughly 9,000–14,000 nanometers or 9–14 μm) and produce images of that radiation, called thermograms. Since infrared radiation is emitted by all objects above absolute zero according to the black body radiation law, thermography makes it possible to see one's environment with or without visible illumination. The amount of radiation emitted by an object increases with temperature; therefore, thermography allows one to see variations in temperature. When viewed through a thermal imaging camera, warm objects stand out well against cooler backgrounds; humans and other warm-blooded animals become easily visible against the environment, day or night. As a result, thermography is particularly useful to military and other users of surveillance cameras. Specialized thermal imaging cameras use focal plane arrays (FPAs) that respond to longer wavelengths (mid- and long-wavelength infrared). The most common types are InSb, InGaAs, HgCdTe and QWIP FPA. The newest technologies use low-cost, uncooled microbolometers as FPA sensors. Their resolution is considerably lower than that of optical cameras, mostly 160x120 or 320x240 pixels, up to 640x512 for the most expensive models. Thermal imaging cameras are much more expensive than their visible-spectrum counterparts, and higher-end models

are often export-restricted due to the military uses for this technology. Older bolometers or more sensitive models such as InSb require cryogenic cooling, usually by a miniature Stirling cycle refrigerator or liquid nitrogen.

A bolometer is a device for measuring the power of incident electromagnetic radiation via the heating of a material with a temperature-dependent electrical resistance. It was invented in 1878 by the American astronomer Samuel Pierpont Langley. The name comes from the Greek word *bole* (βολή), for something thrown, as with a ray of light. Langley's bolometer consisted of two platinum strips covered with lampblack. One strip was shielded from radiation and one exposed to it. The strips formed two branches of a Wheatstone bridge which was fitted with a sensitive galvanometer and connected to a battery. So when resistance of the exposed platinum gets changed there will be current flow in the galvanometer.

A microbolometer is a specific type of bolometer used as a detector in a thermal camera. Infrared radiation of wavelength ranging between 7.5-14 μm strikes the detector material heats it, and thus changes its electrical resistance. This resistance change is measured and processed into temperatures which can be used to create an image. Unlike other types of infrared detecting equipment, microbolometers do not require cooling.

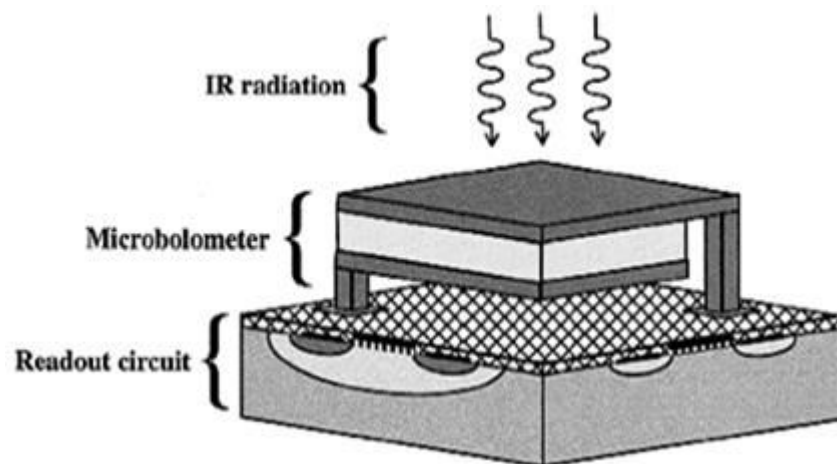


Fig.1.1: Microbolometer and Readout Circuit [1]

As shown above the fig.1.1 shows the microbolometer with its corresponding ROIC as a complete system.

1.2 Motivation

An infrared sensor is an electronic instrument that is used to sense certain characteristics of its surroundings by either emitting and/or detecting infrared radiation. It is also capable of measuring heat of an object and detecting motion. The IR sensor has verity of applications as mentioned below

- Tracking and art history.
- Climatology, meteorology, and astronomy.
- Thermography, communications, and alcohol testing.
- Heating, hyperspectral imaging, and night vision.
- Biological systems, photobiomodulation, and plant health.
- Gas detectors/gas leak detection.
- Water and steel analysis, flame detection.
- Anesthesiology testing and spectroscopy.
- Petroleum exploration and underground solution.
- Rail safety.

Below shown are some pictures taken by microbolometer sensors and their field of applications.



Fig1.2: Night vision mainly used in military.

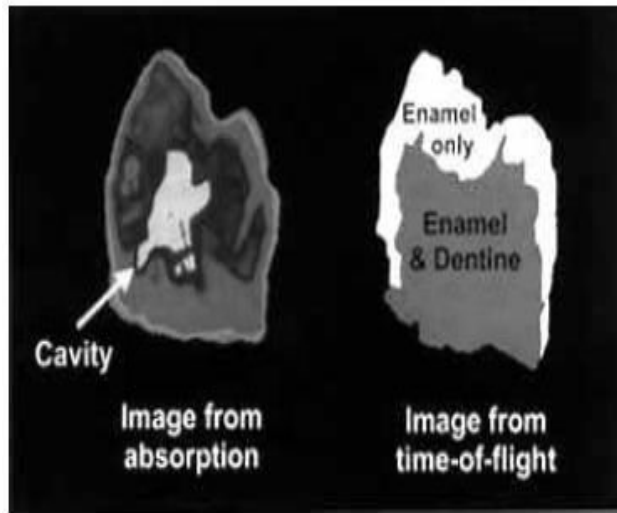


Fig.1.3: Early detection of tooth cavity.

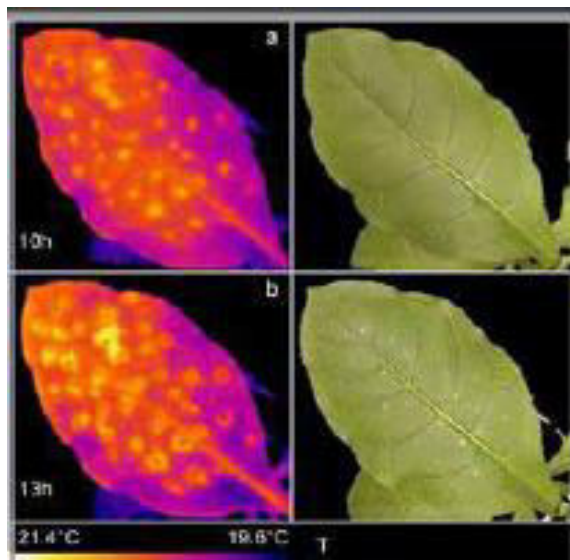


Fig.1.4: Determining net water loss

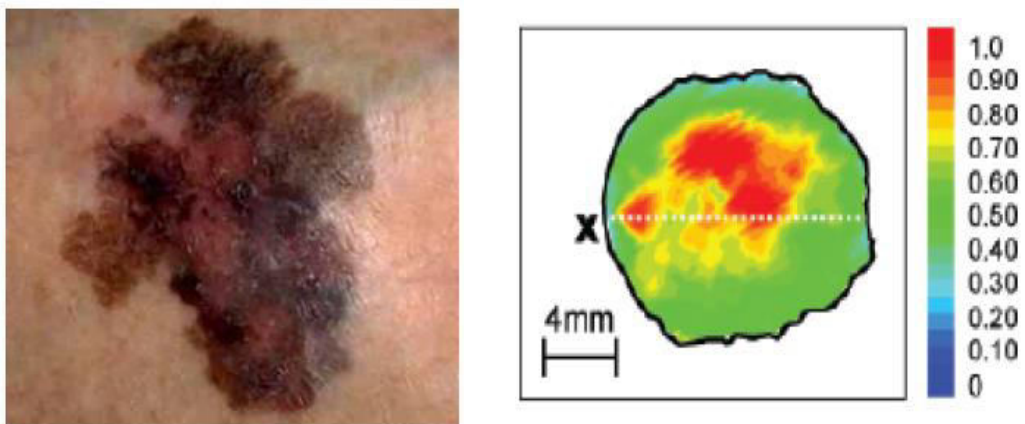


Fig.1.5: Detection of skin cancer

As mentioned above the IR sensor/detector is used in many fields of applications. Hence the quality of image, sensitivity of the device and cost play very important role in different field of applications. For example in astronomy the sensitivity of the device matters more as it has to detect asteroids from distance places but in biomedical applications rather than sensitivity cost matters a lot.

1.3 Aim and objectives of the thesis

Main objective of the thesis was to make the commercial based IR sensor, microbolometer in ultra-low cost and simple method of fabrication. Our aim was initially to make the Microbolometer sensing element using simple process steps and then go for 3D integration of the sensor with its corresponding ROIC, so that the sensing membrane with its ROIC can be available as a complete package. This will be of low cost and efficient IR sensor with considerable reduced effort. While making the microbolometer sensor we also designed Si based microbridges/cantilevers using low cost and simple etching steps.

1.4 Thesis Outline

Before going for bolometer fabrication, a simple Si cantilever/microbridge structure was fabricated, which could be the basic structure for the microbolometer. We started with the traditional electrochemical wet etching process to fabricate the Si microbridges and end up with novel idea to fabricate Si microbridges, which was low cost method to fabricate microbridges. Then this technique is used and tried to fabricate the microbolometer structure which is also of low cost.

So the outline of the thesis comprises of two distinct sections one in which an efficient Si microbridges have been fabricated and second in which efficient microbolometer sensors were fabricated. The detail of the work is put in the chapters shown below which is explained completely in later stages.

- I. Design, Simulation and fabrication of Si based Microbridges/cantilever and array using front end bulk micromachining.
- II. Design optimization by making efficient mask designs to reduce area consumed per microbridge and increase in number of microbridges.

- III. A comparative case study to make Si microbridges using all of the above designs and hence showing the most optimized mask design in fabricating microbridges and micro cantilevers both in terms of area utilization and number of devices.
- IV. Design and Simulation of Microbolometer sensors using two methods
 - 1. Using only wet etching.
 - 2. Using Dry etching followed by wet etching.
 - DRIE followed by TMAH etching.
 - DRIE followed by HNA etching.
- V. A comparative case study between the above mentioned methods of fabricating microbolometer.
- VI. Design optimization by making efficient mask designs to reduce area consumed per pixel of microbolometer.
- VII. Fabricating results of the microbolometer.
- VIII. A comparative case study of area efficient mask designs to make microbolometer.

The detail of the thesis outline presented above is explained in the next chapter with the results.

Chapter 2

LITERATURE SURVEY

2.1 Fabrication of Si Microbridges and Cantilevers

Micro-electro-mechanical systems (MEMS) consist of mechanical components as well as electronic circuits integrated with each other as a complete system. Micro fabrication plays a very important role in miniaturizing the mechanical components as a result of which those devices are capable of integrated with electronics which as a whole system can be implemented in chip giving very good performance. Surface and bulk micromachining [2] are the two most important processes to make mechanical components. Being simple and cost effective way of removing parts of Silicon, anisotropic wet etching is highly demanded in MEMS processes to make different types of sensors and actuators.

Microcantilevers and microbridges are the frequently used structures in many of MEMS devices and simple structures are also used as thermal, mechanical and biomolecule detectors. So the ease and cost of process is highly dependent of the fabrication of those microstructures. There are majorly three methods to fabricate Si Microbridges/cantilevers.

- i. By using a sacrificial layer.
- ii. SOI method.
- iii. Bulk micromachining.

Using a sacrificial layer for making the device causes the ease of fabrication difficult similarly using an SOI wafer makes the cost of the process high. But bulk micromachining of Si to make the microbridge/cantilever is one of the simple and cost effective ways to fabricate the microbridges/cantilevers.

2.2 Microbolometer and Fabrication

Bolometers are nothing but the Heat or IR sensors in which basically the resistance of the device get changed with the absorbed IR radiation. Every living and non-living objects have certain thermal signature, the device is able to detect the object from the IR radiation emitting from it. Hence it has a wide range of applications such as night vision, infrared imaging, biomedical applications such as skin cancer, early tooth cavity detection except these it also used in astronomy and so on. Microbolometers are getting more attention because of its light weight, low cost and low power usage. But the challenge lies in implementing very large format arrays at low cost.

A lot of techniques have been reported so far to fabricate microbolometers and array of it. The most commonly used manufacturing approach for uncooled infrared bolometer FPAs is monolithic integration[3], which is shown below.

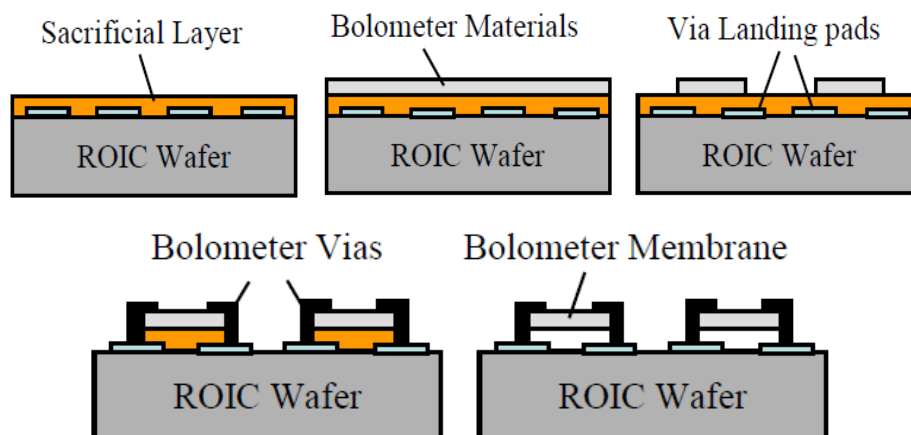


Fig2.1: showing monolithic method of bolometer fabrication [3]

In this method ROIC is pre-manufactured then on top of that a high temperature polyamide is deposited as sacrificial layer. The bolometer material (ex. VOx) is deposited on top of that which is then patterned and bolometer vias are created for contact, then by using oxygen plasma the sacrificial layer is removed which results in free isolated bolometer.

But the disadvantages we observed in this method are

- (1) Some monocrystalline bolometer materials require more than 450 degree centigrade for deposition which may damage our underlying ROIC at that temperature.
- (2) As the structure obtained in this method is hanging without any support so the reliability is the major concern in this method.

The second method of fabrication is the bulk micromachining the fabrication is done in CMOS line after the ROIC is made shown in fig.2.2 [4][5]. In this method of fabrication electrochemical etch stopping technique [6] is used for which there require n-well layers in p-type substrate and those n-wells are used as the sensing elements.fig.2.2 shows the bolometer device obtained using bulk micromachining.

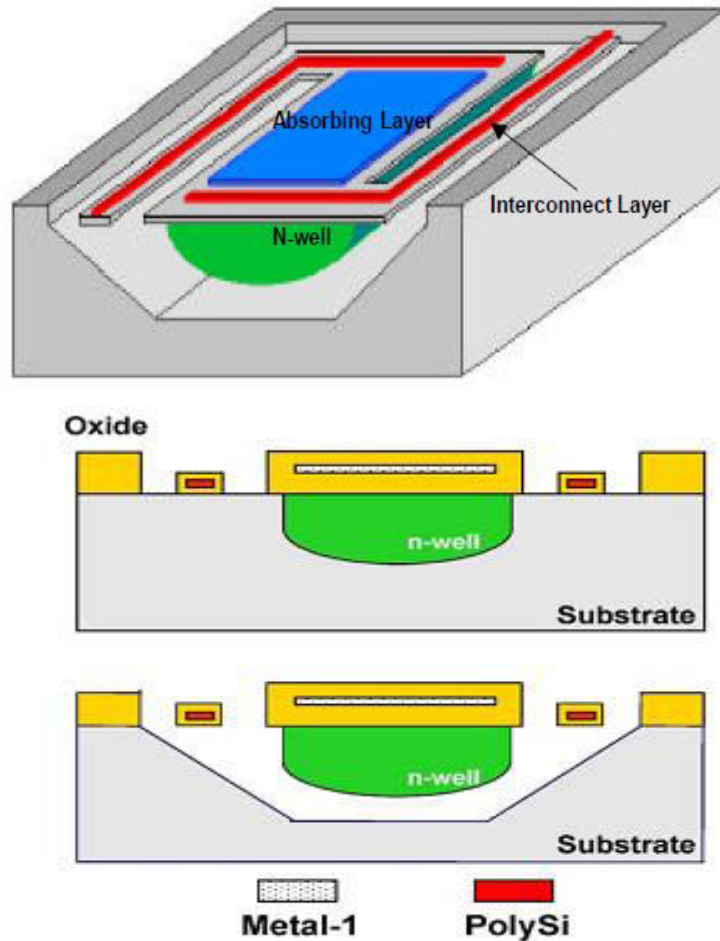


Fig.2.2: showing the front view of CMOS line microbolometer [3]

In this method the bolometer is fabricated in standard CMOS line i.e. first the ROIC is fabricated and after that bulk micromachining is done by electrochemical etching method where an n-well is used as the etch stop layer.

But the disadvantages got in this method are

- (1) The ROIC cannot place beneath the bolometer membrane which reduces the pixel form factor.
- (2) The end step is the electrochemical wet etching step which required potential to apply for the etching to be stopped in sensor membrane which is cumbersome while going for array of bolometers and may not be good for the ROIC.

Then the third important method to fabricate microbolometer is 3D integration [7], which avoids the high temperature issue in monolithic for which it was difficult to put some monocrystalline material on top of ROIC wafer. The process steps are shown in fig.2.3.

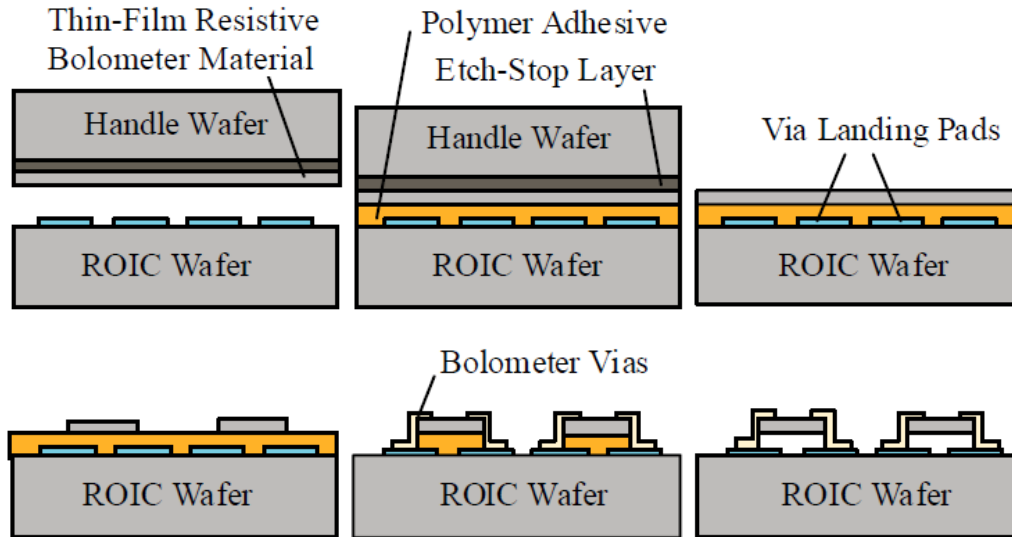


Fig.2.3: showing heterogeneous 3D integration of bolometer

But the issues lying in the above method are

- (1) The method suffers from reliability issue.
- (2) The process is costly as it requires a handle wafer which is normally SOI.

There are a lot of materials proposed to be used as the bolometer material few of which with their temperature coefficient of resistance is put here.

Table-2.1 showing bolometer material with its TCR[3]

Bolometer Material	Temp. coefficient of Resistance(TCR)
VO _x	3% /°k
Amorphous Si(α -Si)	3% /°k
Amorphous Si thin film transistor(TFT)	1.5-6.5%/°k
Titanium	0.35%/°k
Germanium-silicon-oxygen compounds (GexSi1-xOy)	5.1%/°k

Chapter 3

Silicon Bulk micromachining

3.1 Frontend Bulk micromachining to make Si microbridges

Frontend bulk micro machining is one of the proven techniques of making suspended microstructures and is highly adapted due to its simple and cost effective way of fabricating the devices. Here we propose novel geometric mask designs for achieving area efficient microstructures by frontend Si bulk micromachining.

In this work a geometric mask design having a microstructure between two rectangular openings is adopted. These openings are aligned at 45° to wafer prime flat of (100) silicon wafer and act as etch openings for frontend bulk micromachining. Alignment of the mask patterns relative to wafer crystallographic orientation is critical in the fabrication of many MEMS devices.

Etch rate of anisotropic wet etchant varies depending on the crystal plane exposed. Etch rate is lower on more densely packed surface than that of loosely packed surface so etch rate of $(100) > (110) > (111)$. The structure and dimension of the pattern etched on Si substrate depends not only on the orientation of Si substrate but also on geometry of opening, its alignment relative to wafer's crystal axes and the duration of etching [10]. Fig.3.1 shows the Si wet etch in (100) wafer where the mask is aligned in (110) direction. As shown the etched pattern obtained is bounded by four (111) planes and all those four planes make an angle of 54.7° with respect to the surface plane. But if we make the mask aligned in the (100) direction in (100) wafer then there can be seen significant undercut inside the mask layer. Si is not only etched in vertical direction but also etched in horizontal direction as all of the exposed planes are (100) in nature[14]. Fig.3.2 shows the etching in (100) wafer where mask oriented in (100) direction.

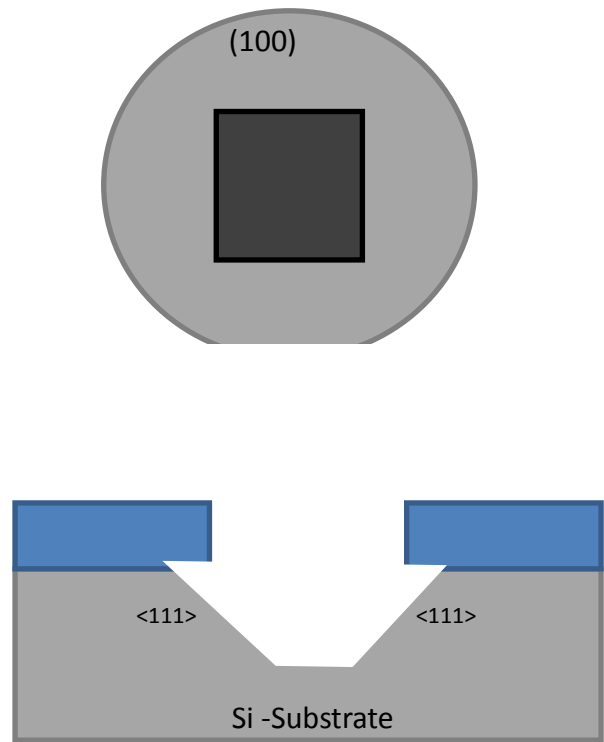


Fig.3.1: showing etching in (100) plane with the shown mask orientation with respect to wafer flat.

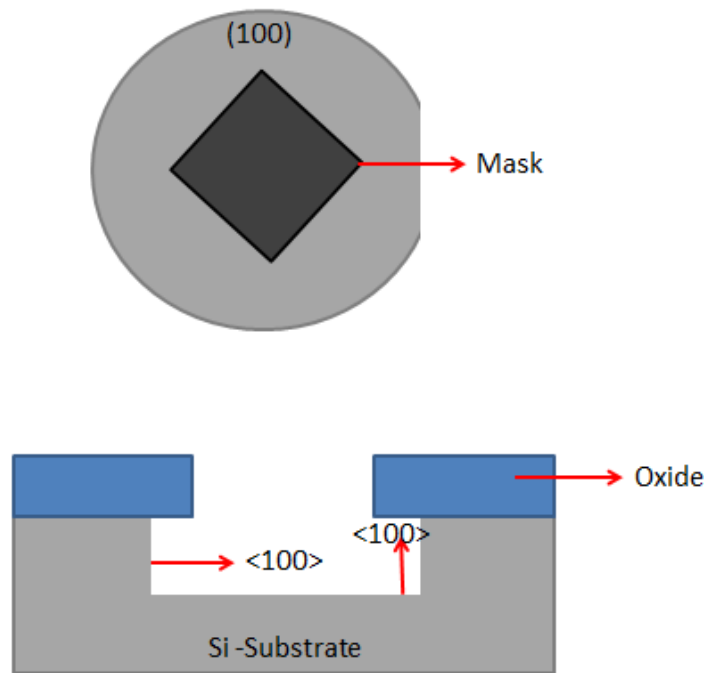
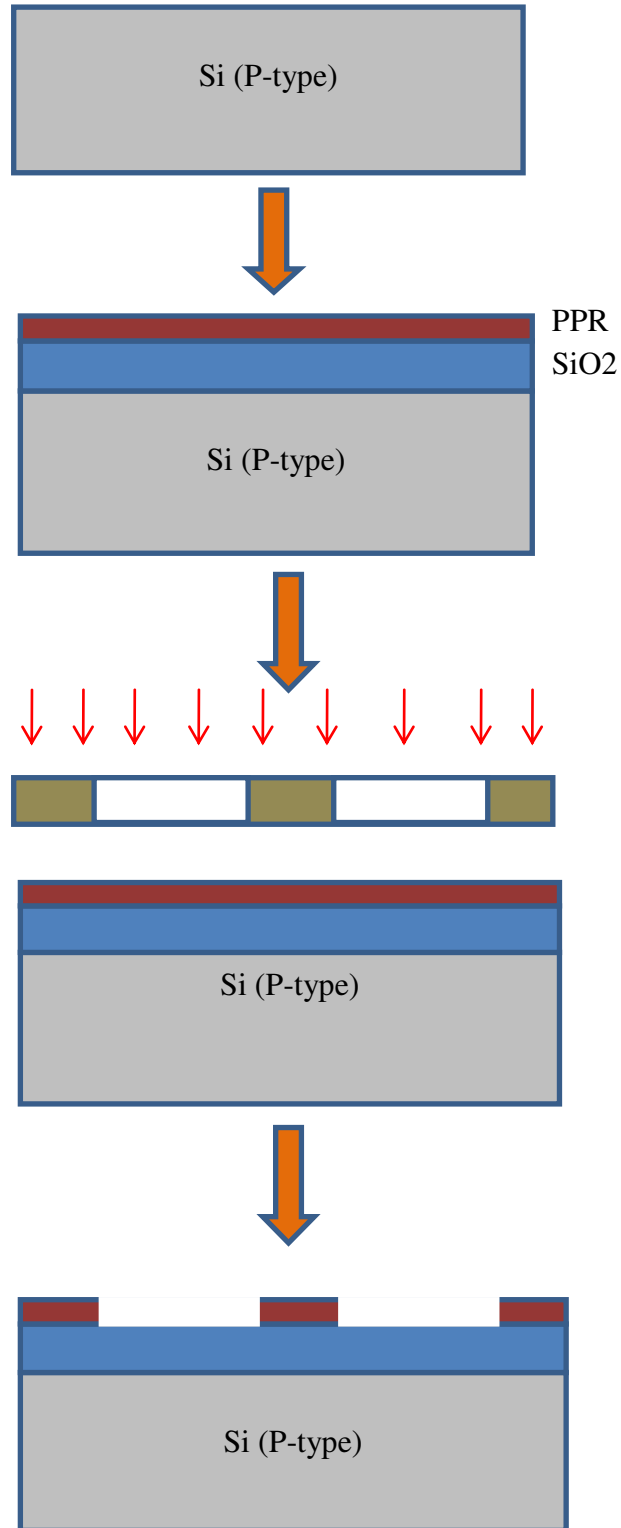
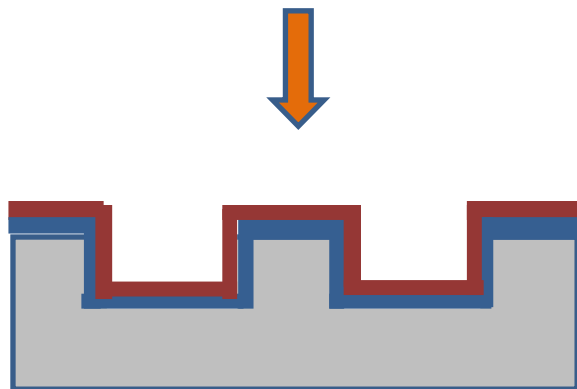
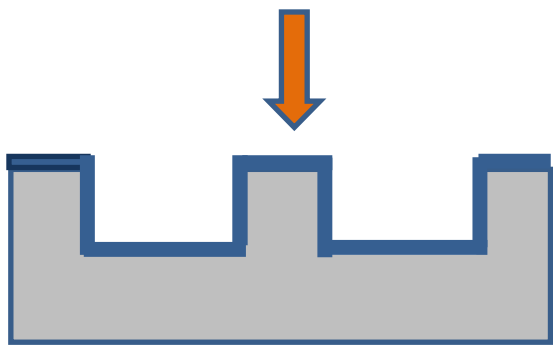
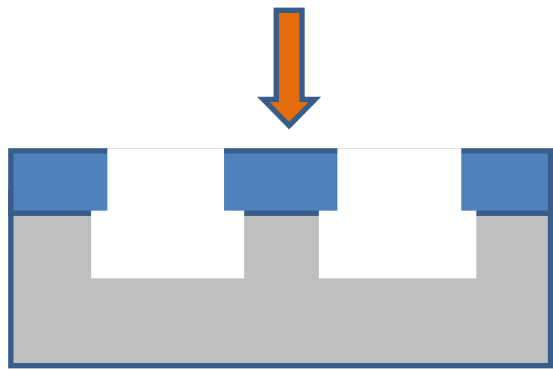
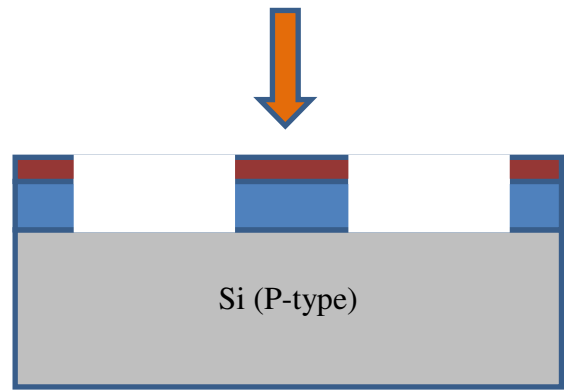


Fig. 3.2: Etched pattern obtained in (100) Si wafer with mask aligned in (100) direction.

3.2 Process flow for obtaining Si microbridge

The process flow for making the cantilevers is as shown below.





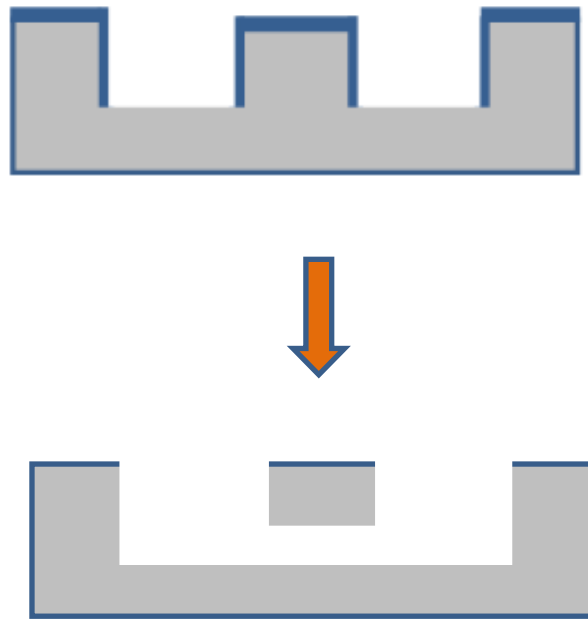


Fig.3.3: Process flow for making Si Bridge.

3.3 Results and Discussion

We made the desired mask and carried out the experiment to see the etched profile obtained in (100) wafer, when the mask is in (100) direction. Fig.3.4 shows wafer after 1st etching step and fig.3.5 and fig.3.6 shows optical profilometer images showing the plot of height versus width of the etched pillar obtained after the first etching. If the etching is done in both the direction then by controlling the time of etching and hence etches depth we can have Si cantilevers and bridges in only two step etching process but we need to protect the sidewalls of the etched pillars after first etching step.

We started the process with taking Si (100) wafer, oxidized it where the oxide acts as the etch mask. Made the mask and rotated it by 45° so that while exposing the mask will be in the direction of (100) plane. Then by using anisotropic etchant TMAH we etched the Si to the depth of 8μm. In the subsequent step we cleaned the etched wafer oxidised it. Using the same mask once again we exposed and etched to a depth of 16μm which results in the formation of Si cantilever/Bridge. The above process is simulated in FABSIM which is shown in Fig. 3.7.

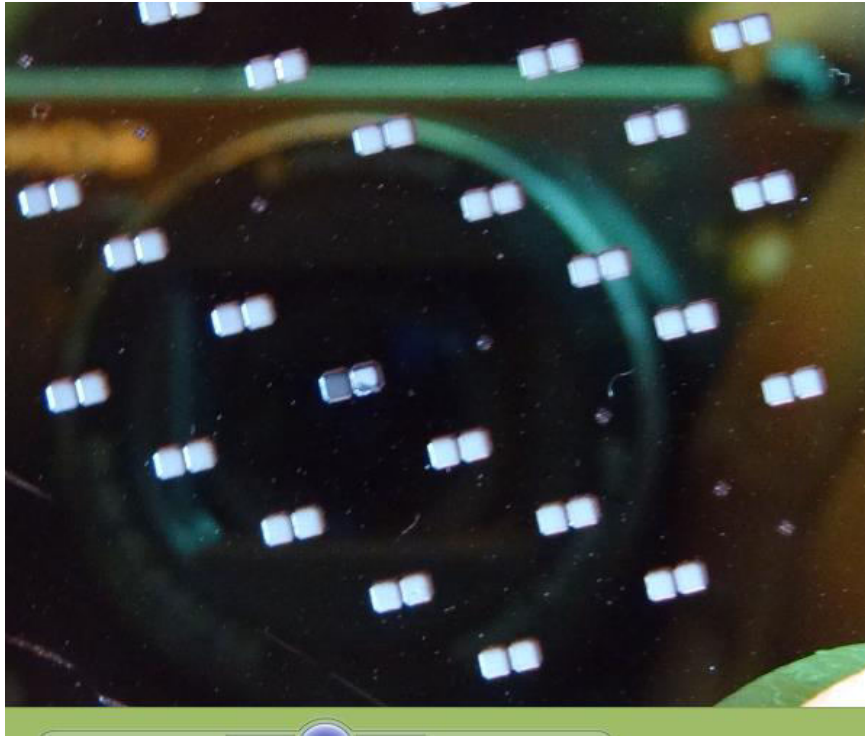


Fig.3.4 showing wafer after 1st etching step

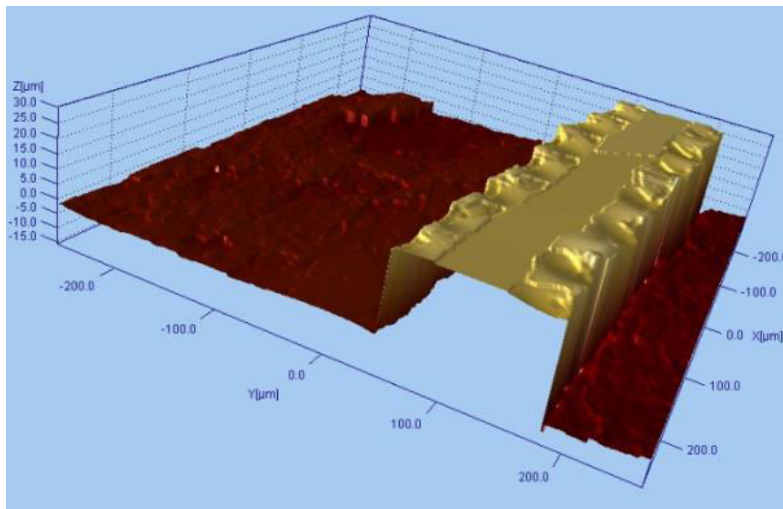


Fig. 3.5: The optical profilometry image of the etched pattern obtained where mask is in (100) direction

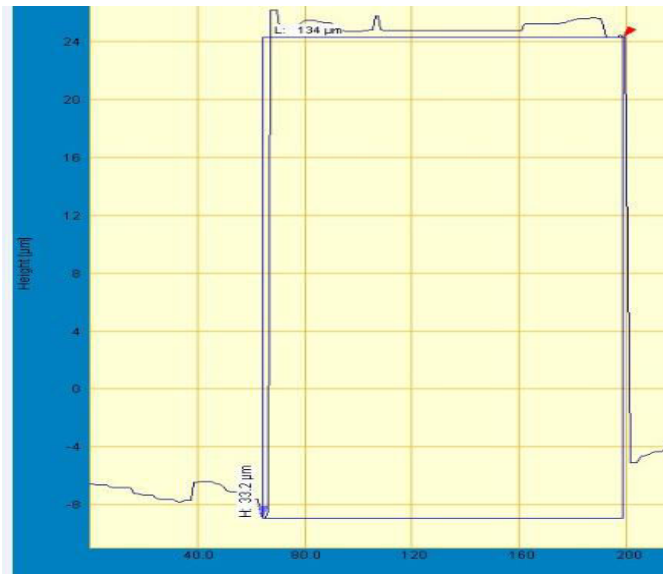


Fig. 3.6: Height and width of the etched pillar after first etching step.

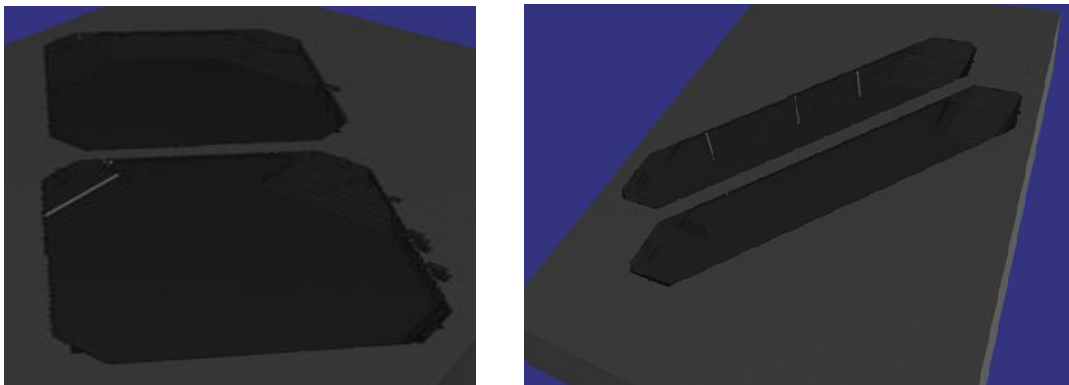


Fig.3.7.FABSIM based physical simulation for making Si micro bridge.

This is the most simple method of making Si microbridges by using only chemical etchant. But as we can observe from the result, for making we are wasting a lot of area being etched outside which is due to opening created by the mask. So to avoid this issue we go for some area efficient mask designs which is explained in the next section.

Chapter 4

Simulation and Fabrication of Si microbridges

4.1 Proposed Method to reduce area consumption for making Si Microbridges.

In the previous design the rectangular openings lead to high silicon area consumption which makes the process unworthy. Therefore we proposed different geometries to minimize area consumption for achieving the same dimension of suspended structure. All these different geometries are simulated using Intellisuite FABSIM based physical simulator. We have observed more than 28% reduction in foot print over literature reported design.

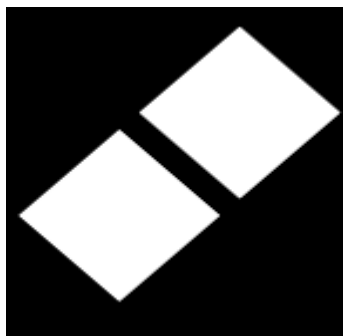


Fig.4.1 showing mask for basic microbridge obtained.

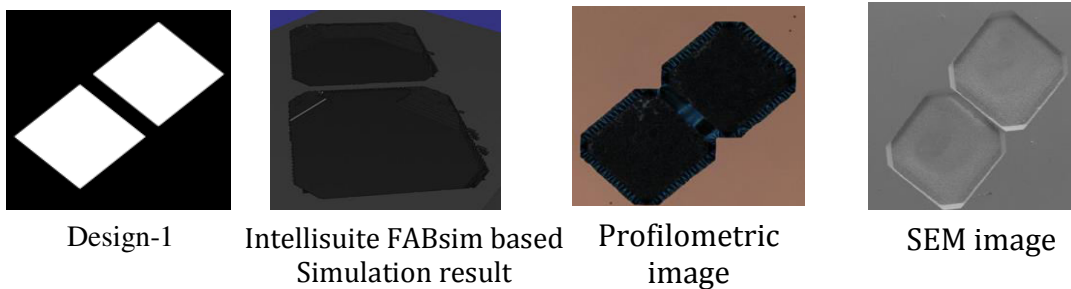
Fig.4.1 shows the mask used to create the Si micro bridge, where there are two rectangular openings. Those openings expose all the planes which are (100) in nature but out of all the (100) planes only one per opening is used to make the bridge. All other exposed (100) planes contributed to unnecessary etching outside the concerned area which increases foot print of each micro bridges. So to reduce the area consumed per device, we cut the mask used in previous case by half as shown in design-2. Now by doing this we have exposed only two (100) planes and one (111) plane which reduces the area consumed per pixel of Si bridge by more than half than the previous case. Once again the area utilized per device can be reduced if we make the mask as shown in Design-3, where we reduced the openings for etchant to enter. But it can be observed from design-3 that, unnecessarily we are creating extra openings in the mask for the etchant

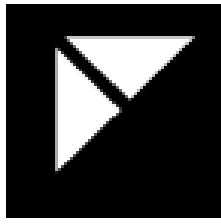
where the device will not present. These areas can be saved if we cut half the portion of the mask as shown in Design-4. The mask gives advantage of opening only one (100) plane in the direction the device is present except which the etching in other directions is insignificant. This design is one of the most area efficient designs to make the Si micro bridges.

Another approach to minimize the area consumption per pixel also presented here. Where we halved each triangular opening shown in Design-2 in such a way that they will expose only one (100) plane and two (111) planes as shown in Design-5. As a result of which outside etching is prevented to happen because of (111) plane and there will be only inside etching due to (100) plane. Now if we want to reduce the area per pixel then we can go for the mask as shown in Design-6, where we reduced the opening for etchant to enter. Design-7 is made by bringing closer two same designs of category design-2. We are getting two advantages out of it. First all the outside planes are (111) in nature hence reduces underetch outside of concerned area and instead of getting only one microbridge, we are getting four microbridges. Now by design-8 we have reduced the opening for wet etchant which reduces area consumption further.

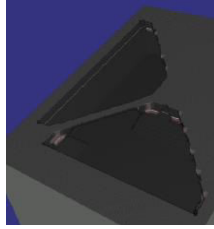
4.2 Simulation and Fabrication of Area efficient Si microbridges

We carried the FABSIM based physical simulation by considering all those masks which we put in fig.4.2. Each of the mask designs produce the same cantilever but the results obtained considering different mask designs gives a clear cut comparison of the area savings.

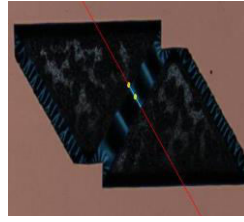




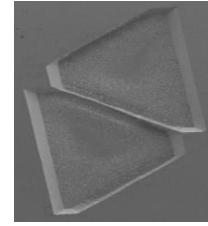
Design-2



Intellisuite FABsim based Simulation result



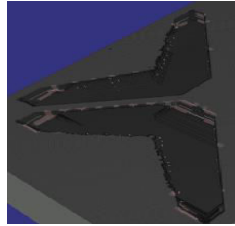
Profilometric image



SEM image



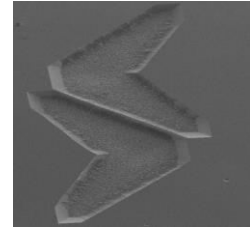
Design-3



Intellisuite FABsim based Simulation result



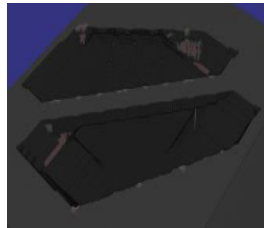
Profilometric image



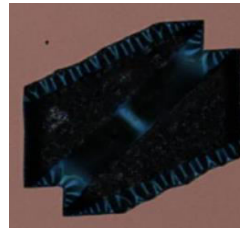
SEM image



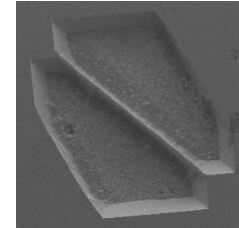
Design-4



Intellisuite FABsim based Simulation result



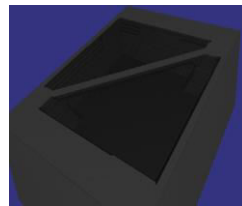
Profilometric image



SEM image



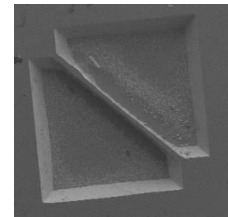
Design-5



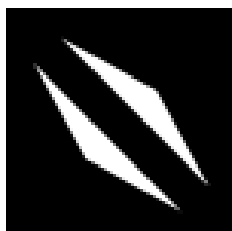
Intellisuite FABsim based Simulation result



Profilometric image



SEM image



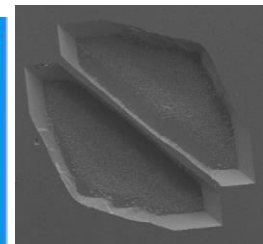
Design-6



Intellisuite FABsim based Simulation result



Profilometric image



SEM image

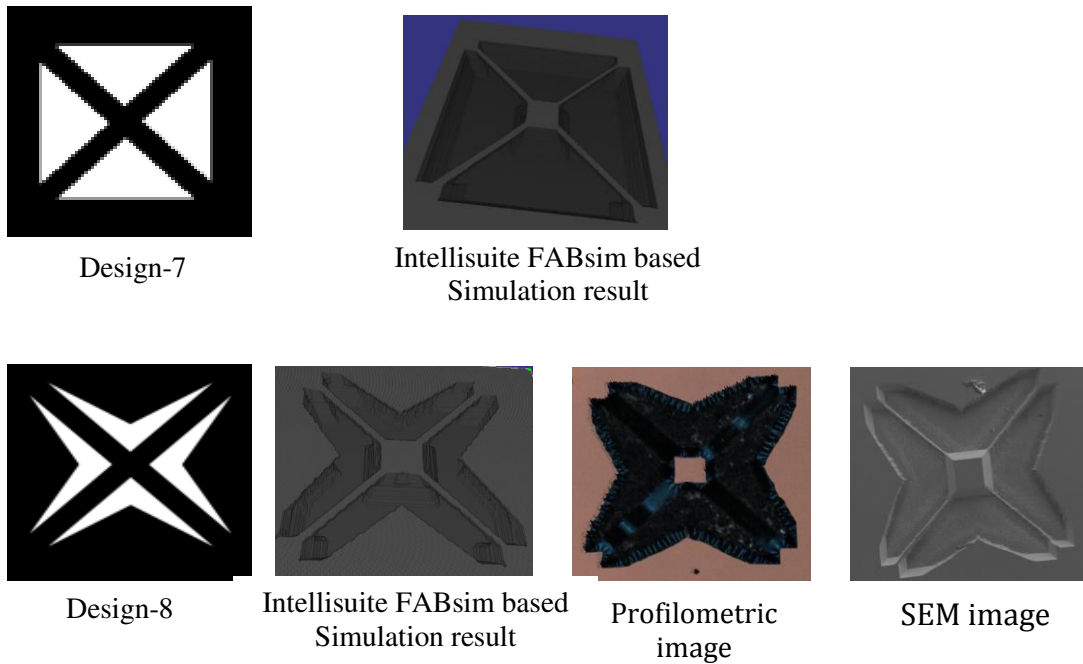


Fig. 4.2 showing all the designs along with intellisuite FABSIM simulations, optical profilometry images and their corresponding SEM images.

The following fig.4.3 shows the cantilever beams. Where after Si microbridges formed, by using another mask we etched the middle connecting island which gives rise to freely hanging isolated cantilever beams. This has implemented using mask design-7 and simulated using Intellisuit based FABSIM physical simulator.

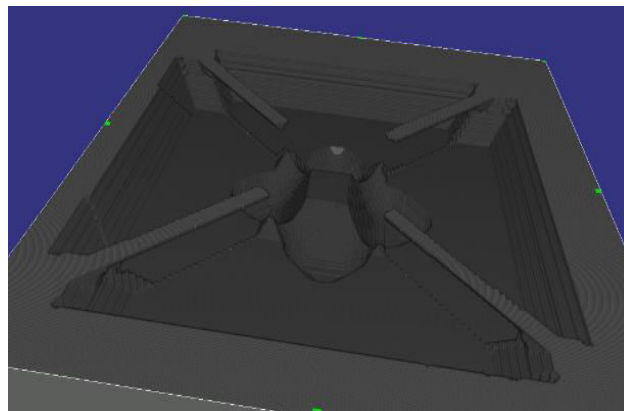


Fig.4.3: Showing cantilever beams through Intellisuit FABSIM based physical simulation.

4.3 Comparative case study of all the area efficient mask designs

Table-1 shows comparison of area consumption in making a microbridge and observed that almost 80% area saving as compare to basic design and about 28% as compared to design-4 which happened to be similar to Fang¹ reported design. Additionally we designed and simulated four leg microbridge and four cantilevers by front end bulk micromachining by using the above mention concepts. This finding will be useful to fabricate cost effective and area effective different MEMS suspended structure in Si used in various sensors application.

TABLE-4.1

Showing the comparison of all the mask design presented

Designs	Opening area per mask	Outside Exposed (100) planes per mask	Number of beams generated	Total area consumed theoretically	Total area consumed from simulation (in sq. μm)	Remarks based on foot print per device
Design-1	A [#]	6	1	A+6 σ ^{\$}	111950	Poor
Design -2	A/2	2	1	A/2+2 σ	46326	Average
Design -3	A/2-2X*	2	1	A/2-2X+2 σ	37953	Good
Design -4	A/4	0	1	A/4	31708	Good
Design -5	A/4-X	0	1	A/4-X	25486	Very good
Design -6	A/4-X	0	1	A/4-X	22823	Very good
Design -7	A	0	4	A	29161	High
Design -8	A-4X	0	4	A-4X	22141	Excellent

[#]=Opening area per mask, ^{*}(X= saved area per opening), ^{\$}=etch in (100) plane

Chapter 5

Microbolometer and Design

5.1 Innovative method for fabricating Microbolometer

A lot of techniques have been reported so far to fabricate microbolometers and array of it. But all the methods reported have certain drawbacks e.g. pixel form factor, cost and temperature. We are reporting a technique in which the silicon itself is a bolometer sensing material as that in the case of CMOS line bolometer but unlike CMOS type, here the same silicon substrate is used as the sensing material, may be n-type or p-type depending on the substrate we have chosen, hence avoiding the diffusion step which is required for etch stopping in standard CMOS line bolometer. We are targeting to achieve the array of bolometer by 3D integration technique unlike the usual 3D integration where a sacrificial layer is required which may suffer from the reliability issue of being the hanging structure. Here we are reporting an innovative way of fabricating Bolometer device only by front end bulk micromachining where neither diffusion nor the cumbersome electrochemical etch stopping is required. The thermally insulated membrane achieved can be used as the bolometer sensing material and if we want to increase the sensitivity we can deposit any of the high TCR material such as VO_x over the membrane before going for 3D integration with the ROIC. As the membrane itself is the part of the silicon substrate it is going to give much better reliability as compared to the recently developed heterogeneous 3D integration of bolometer.

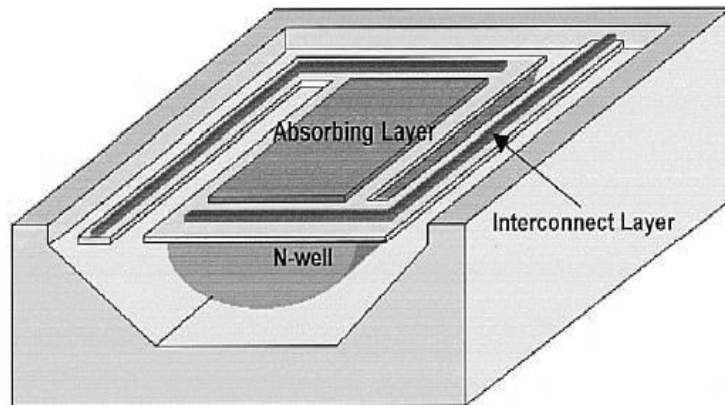


Fig.5.1: showing the standard CMOS line Bolometer fabrication where n-well is used as the sensing layer.

5.2 Process Simulation showing Microbolometer Fabrication using only Front end Bulk micromaching

We adopted mainly two fabrication processes for microbolometer sensor . One involving only wet etching of Si and in the other, dry etching followed by wet etching. Both the processes have been described here. In both the methods, we started with oxidised Si wafers, made the desired mask for bolometer sensor and rotated it by 45° before printing as the primary step. Every part of the mask is nothing but a rectangular structure, so rotating it with 45 degree and putting in TMAH will result in vertical etching , as all the (100) planes are exposed inside.

5.2.1 Only using wet etching

Fabrication using only chemical etching started with a mask dimension of $128\mu\text{m}$ length and $60\mu\text{m}$ width. To make the process more cost effective only one mask is used in the entire process. At first we exposed the spin coated Si wafer with the mask and etched for 9000nm . Then the resulting etched wafer is put in oxidation chamber to get oxidized. As the TMAH etching is done both in horizontal as well as vertical direction, etching started exposing the (111) planes as it goes in horizontally, those exposed (111) planes creates problem by restricting the etching in that direction. So we have removed these exposed (111) planes using isotropic etchant HNA (HNO_3+HF) by etching to a depth of 7600nm . After isotropic etching the wafer is cleaned and then again oxidized. Now in the final step the resulting etched Si wafer is again etched using anisotropic wet etchant TMAH, which

results in the formation of freely standing isolated membrane which can be used as the sensor for microbolometer. In the whole process we have used only one mask for exposing under UV. The process flow of the above method is shown in the fig.5.2.

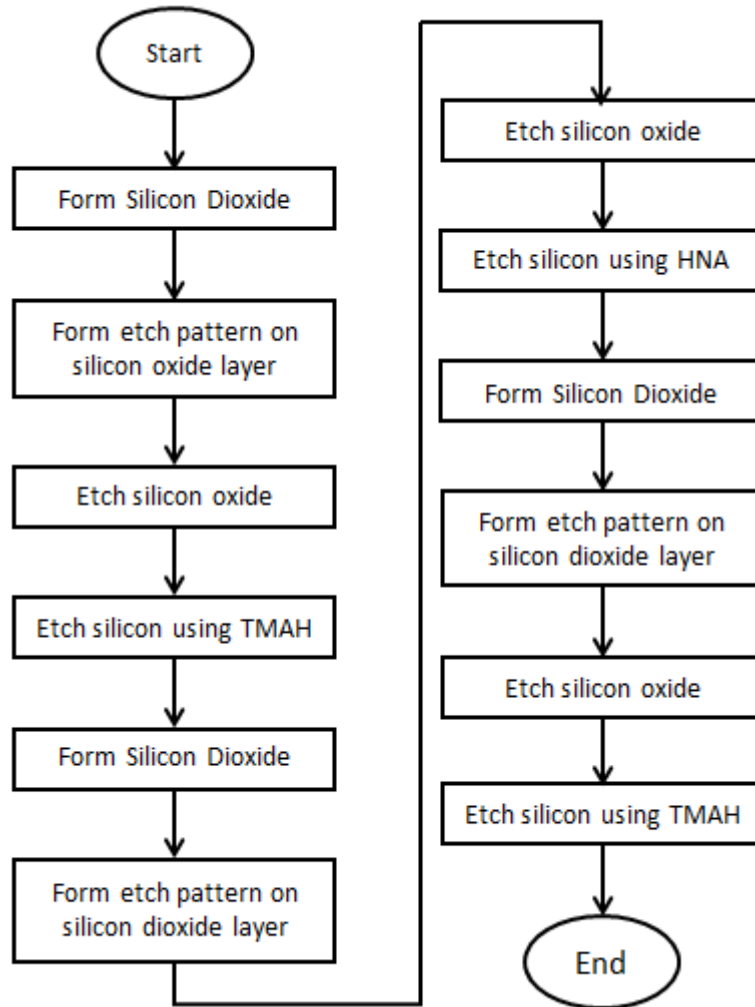


Fig.5.2: showing process flow to obtain microbolometer sensor.

5.2.1.1 Simulation Results

The above process is simulated using Intellisuite FABSIM based physical simulator. Fig.5.3 shows the basic mask design used for the above method and simulation result showing sensor membrane. Fig.5.4 shows the process table used to make the above sensor membrane.



Fig.5.3: showing the mask used and the bolometer sensor membrane obtained using Intellisuite based FABSIm physical simulation.

1	Definition	Si	Czocharalski	100	
2	Etch	Si	Clean	RCA	
3	Deposition	SiO2	Thermal	Wet	Conformal Deposition
4	Etch	Si	Clean	RCA	
5	Etch	Si	Clean	Piranha	
6	Deposition	PR-S1800	Spin	SI813	Conformal Deposition
7	Exposure	UV	Contact	Suss	
8	Etch	SiO2	Wet	BHF	Partial Etching
9	Etch	PR-S1800	Wet	1112A	Partial Etching
10	Etch	Si	Wet	TMAH	Partial Etching
11	Etch	SiO2	Wet	BHF	Partial Etching
12	Etch	Si	Clean	Piranha	
13	Deposition	SiO2	Thermal	Wet	Conformal Deposition
14	Etch	Si	Clean	RCA	
15	Etch	Si	Clean	Piranha	
16	Deposition	PR-S1800	Spin	SI813	Conformal Deposition
17	Exposure	UV	Contact	Suss	
18	Etch	SiO2	Wet	BHF	Partial Etching
19	Etch	PR-S1800	Wet	1112A	Partial Etching
20	Etch	Si	Wet	TMAH	Partial Etching
21	Etch	Si	Wet	HNO3_HF	Partial Etching
22	Etch	SiO2	Wet	BHF	Partial Etching
23	Etch	Si	Clean	Piranha	
24	Deposition	SiO2	Thermal	Wet	Conformal Deposition
25	Etch	Si	Clean	RCA	
26	Etch	Si	Clean	Piranha	
27	Deposition	PR-S1800	Spin	SI813	Conformal Deposition
28	Exposure	UV	Contact	Suss	
29	Etch	SiO2	Wet	BHF	Partial Etching
30	Etch	PR-S1800	Wet	1112A	Partial Etching
31	Etch	Si	Wet	TMAH	Partial Etching
32	Etch	SiO2	Wet	BHF	Partial Etching
33	Etch	Si	Clean	Piranha	

Fig.5.4: showing process table for the above method.

5.2.2 Dry etching followed by Wet etching

5.2.2.1 DRIE followed by TMAH etching

In this method of making microbolometer sensor, dry etching was adopted in the first step which was DRIE (Deep Reactive Ion Etching) then wet etching was carried out using TMAH.

We started with the mask for targeting to make microbolometer sensor of dimension $20\mu\text{m}\times 20\mu\text{m}$ and length of the sensor as $5\mu\text{m}$. The 1st etching step was done to a depth of $10\mu\text{m}$ by using DRIE and the 2nd etch step to a depth of around $15\mu\text{m}$ by using anisotropic wet etchant TMAH. Because of the mask orientation, TMAH etch in horizontal direction along with vertical giving freely hanging and isolated Si membrane which can be used as microblometer sensor. Here we have used two masks for making the sensor membrane unlike of the previous method, where one is used for creating opening for dry etching and second for creating opening for wet etching. Fig.5.5 shows the process flow to obtain microbolometer using above method.

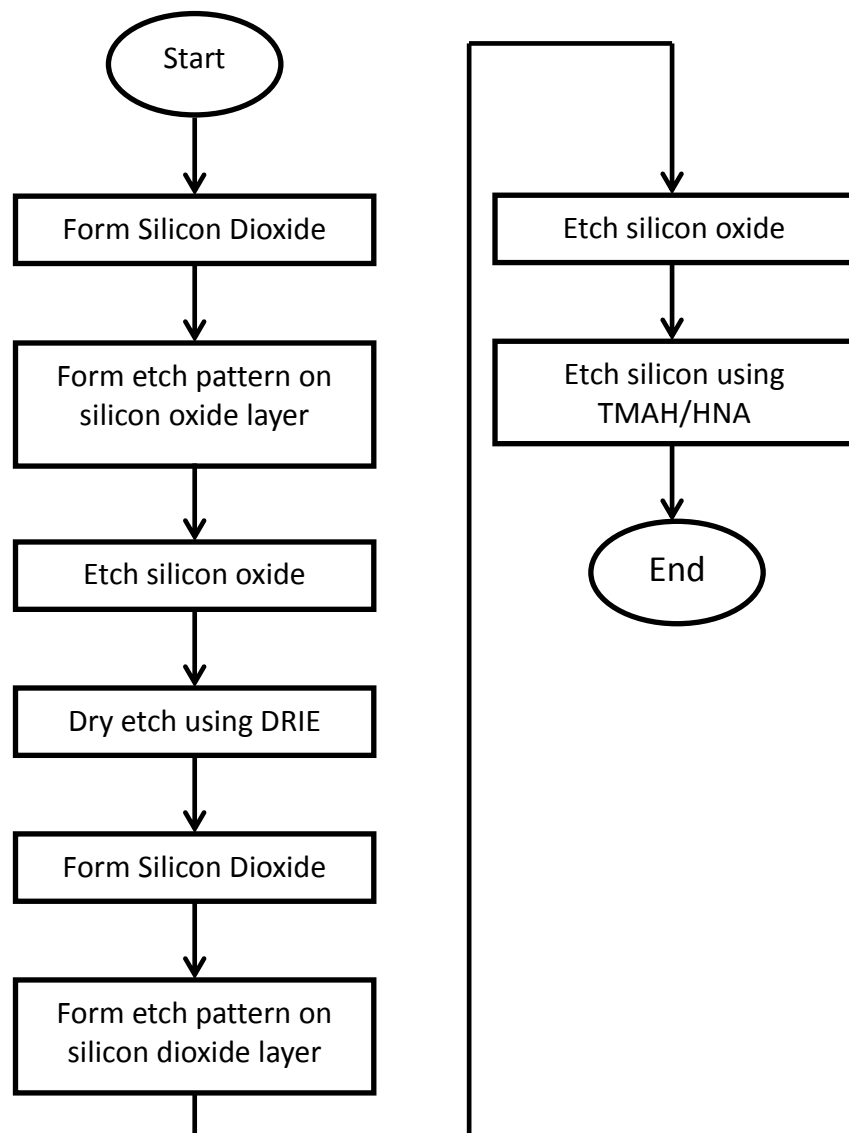


Fig.5.5: shows process flow to obtain Microbolometer using above method.

5.2.2.1.1 Simulation results

The above process is simulated using Intellisuite FABSIm based physical simulator. Fig.5.6 shows the mask used for the above method, simulation result showing sensor membrane and fig.5.7 shows the process table used to make the above sensor membrane.

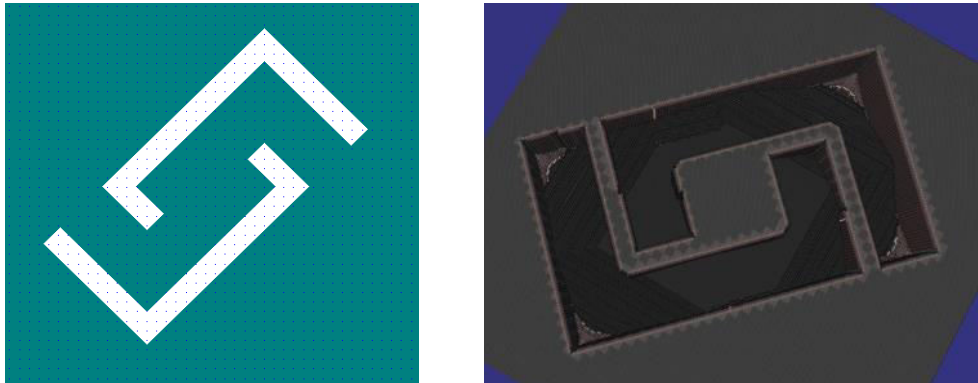


Fig.5.6: showing the mask used and the bolometer sensor membrane obtained using Intellisuite based FABSIm physical simulation.

1	<input checked="" type="checkbox"/>	Definition	Si	Czochralski	100	
2	<input checked="" type="checkbox"/>	Etch	Si	Clean	RCA	
3	<input checked="" type="checkbox"/>	Deposition	SiO2	Thermal	Wet	Conformal Deposition
4	<input checked="" type="checkbox"/>	Etch	Si	Clean	RCA	
5	<input checked="" type="checkbox"/>	Etch	Si	Clean	Piranha	
6	<input checked="" type="checkbox"/>	Deposition	PR-S1800	Spin	SLB13	Conformal Deposition
7	<input checked="" type="checkbox"/>	Exposure	UV	Contact	Suss	
8	<input checked="" type="checkbox"/>	Etch	SiO2	Wet	BHF	Partial Etching
9	<input checked="" type="checkbox"/>	Etch	PR-S1800	Wet	1112A	Partial Etching
10	<input checked="" type="checkbox"/>	Etch	Si	DRIE	SF6_C4F8	Partial Etching
11	<input checked="" type="checkbox"/>	Etch	SiO2	Wet	BHF	Partial Etching
12	<input checked="" type="checkbox"/>	Etch	Si	Clean	Piranha	
13	<input checked="" type="checkbox"/>	Deposition	SiO2	Thermal	Wet	Conformal Deposition
14	<input checked="" type="checkbox"/>	Etch	Si	Clean	RCA	
15	<input checked="" type="checkbox"/>	Etch	Si	Clean	Piranha	
16	<input checked="" type="checkbox"/>	Deposition	PR-S1800	Spin	SLB13	Conformal Deposition
17	<input checked="" type="checkbox"/>	Exposure	UV	Contact	Suss	
18	<input checked="" type="checkbox"/>	Etch	SiO2	Wet	BHF	Partial Etching
19	<input checked="" type="checkbox"/>	Etch	PR-S1800	Wet	1112A	Partial Etching
20	<input checked="" type="checkbox"/>	Etch	Si	Wet	TMAH	Partial Etching
21	<input checked="" type="checkbox"/>	Etch	SiO2	Wet	BHF	Partial Etching
22	<input checked="" type="checkbox"/>	Etch	Si	Clean	Piranha	

Fig.5.7: showing process table for the above method.

5.2.2.2 DRIE followed by HNA etching

This method is similar to that of previous method except of using isotropic etchant HNA instead of anisotropic etchant TMAH in the 2nd etching step.

5.2.2.2.1 Simulation Results

The above process is simulated using Intellisuite FABSsim based physical simulator. The below fig.5.8 shows the mask used for the above method, simulation result showing sensor membrane and the process table used to make the above sensor membrane.



Fig.5.8: showing the mask used and the bolometer sensor membrane obtained using Intellisuite based FABSsim physical simulation

Chapter 6

Efficient Method to Fabricate Microbolometer

6.1 Design and Simulation of area efficient Microbolometers

The mask used in the previous chapter to make the microbolometer sensor is made up of all rectangular areas which when exposed on Si wafer will open all the (100) planes inside as well as outside. Due to which we will not only have undercut inside but also will lose area outside which needs to be prevented. More the area consumed by the sensor, less will be the pixel fill factor. So to reduce the area consumption, we have made some designs which will allow the etchant to enter only in the desired direction and prevent unnecessary area consumption in all other directions. Those mask designs are useful in both the methods of fabricating the microbolometer sensor which has been described neatly in the below subsections. We have proposed four mask designs to reduce the area consumed per pixel of microbolometer sensor. The same concept has been applied to make an area-efficient microbolometer as that of making area-efficient Si microbridges. Below are the explanations of all mask designs.

Design-1 :

This is the basic mask design used to make microbolometer sensor. The openings in this design are all rectangular in nature.

Design-2 :

The mask area opened for etchant in Design-1 can be reduced by cutting down as shown in the figures. As in Design-2 the area of opening is reduced to half of that of Design-1, so area consumption due to outside etching is also reduced.

Design-3 :

In this design we replace the rectangularly opened mask by a number of elemental right-angled triangular structures. While rotating the mask by 45° , the sides of each triangle will expose (111) planes and the hypotenuse will expose (100) plane. Hence the etching in outside will be reduced significantly.

Design-4 :

In this design we cut the rectangular region in Design-1 into triangular region as shown in the figure. The mentioned design is also helpful in saving area due to outside etching.

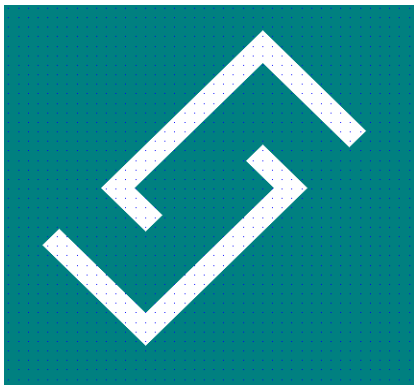
Design-5 :

In this design instead of one triangle as in Design-4 we are going for two triangular regions as shown in the figure. This also helpful in reducing area consumption due to outside etching.

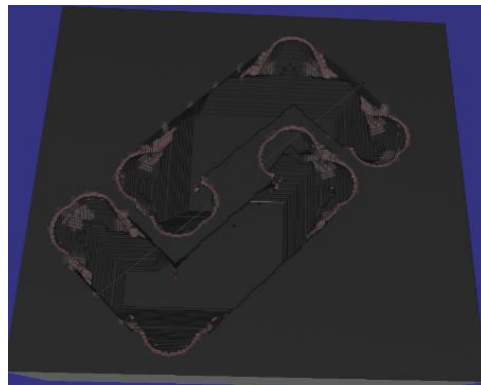
Below presented all the mask designs with their corresponding Intellisuite based FABSIM simulation results.

6.1.1 Only using wet etching

As in previous chapter in this method we are going to use only wet chemical etchants to make microbolometer sensors. Fig.6.1 shows the Designs with corresponding simulation results to obtain microbolometer sensor and table showing length and width per each pixel.



Design-1



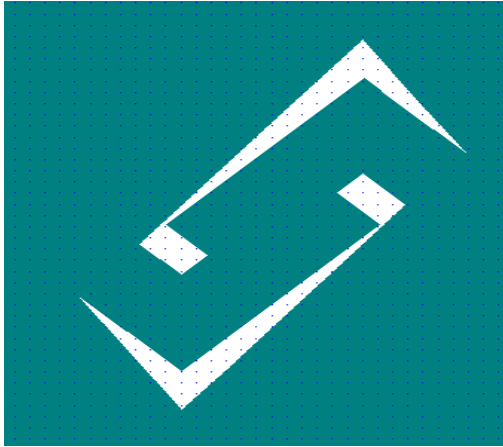
Simulation result in Fabsim

Measure Result:	
Absolute Distance :	<input type="text" value="150.212"/> um
Vertical Distance :	<input type="text" value="0.206524"/> um
Horizontal Distance :	<input type="text" value="150.212"/> um
Elevation Angle:	<input type="text" value="0.0787751"/> deg

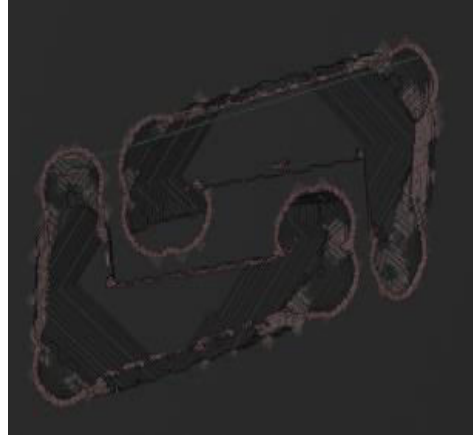
Length of the pixel

Measure Result:	
Absolute Distance :	<input type="text" value="80.5221"/> um
Vertical Distance :	<input type="text" value="1.07586"/> um
Horizontal Distance :	<input type="text" value="80.5149"/> um
Elevation Angle:	<input type="text" value="0.765554"/> deg

Width of the pixel



Design-2



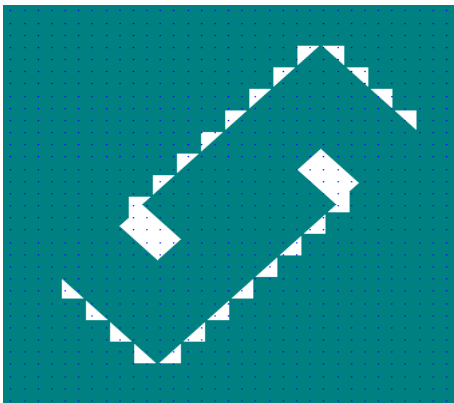
Simulation result in Fabsim

Measure Result	
Absolute Distance :	<input type="text" value="135.848"/> um
Vertical Distance :	<input type="text" value="0.592571"/> um
Horizontal Distance :	<input type="text" value="135.846"/> um
Elevation Angle :	<input type="text" value="0.249927"/> deg

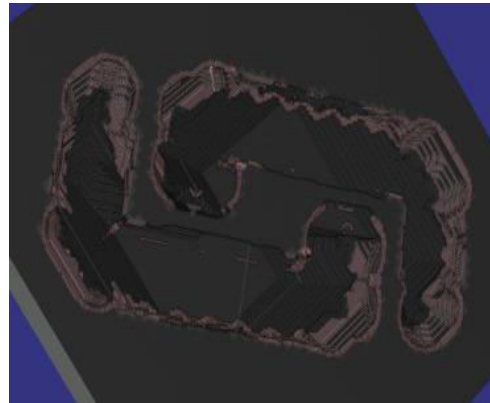
Length of the pixel

Measure Result	
Absolute Distance :	<input type="text" value="75.7496"/> um
Vertical Distance :	<input type="text" value="36.9606"/> um
Horizontal Distance :	<input type="text" value="66.1205"/> um
Elevation Angle :	<input type="text" value="29.2047"/> deg

Width of the pixel



Design-3



Simulation result in Fabsim

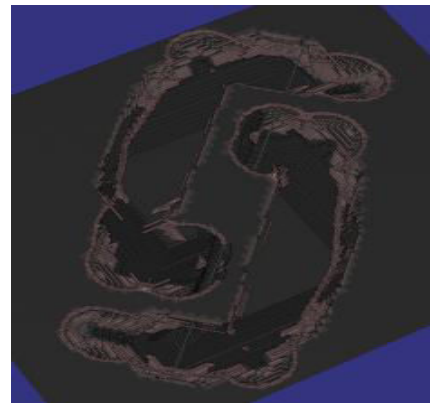
Measure Result

Absolute Distance :	<input type="text" value="23.2777"/>	um
Vertical Distance :	<input type="text" value="0.0129814"/>	um
Horizontal Distance :	<input type="text" value="23.2777"/>	um
Elevation Angle:	<input type="text" value="0.0319524"/>	deg

Start Measure OK



Design-4



Simulation result in Fabsim

Measure Result

Absolute Distance :	<input type="text" value="134.137"/>	um
Vertical Distance :	<input type="text" value="0.140137"/>	um
Horizontal Distance :	<input type="text" value="134.137"/>	um
Elevation Angle:	<input type="text" value="0.0598587"/>	deg

Start Measure OK

Length of the pixel

Measure Result

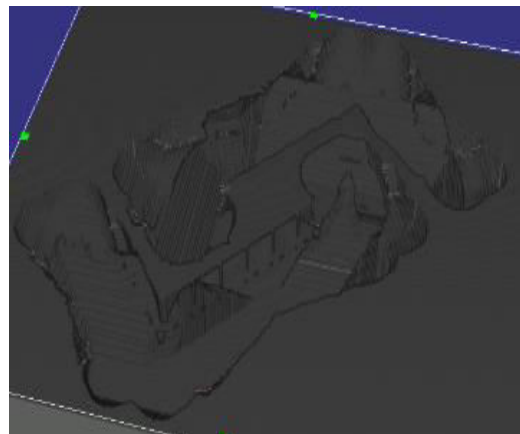
Absolute Distance :	<input type="text" value="67.8772"/>	um
Vertical Distance :	<input type="text" value="0"/>	um
Horizontal Distance :	<input type="text" value="67.8772"/>	um
Elevation Angle:	<input type="text" value="0"/>	deg

Start Measure OK

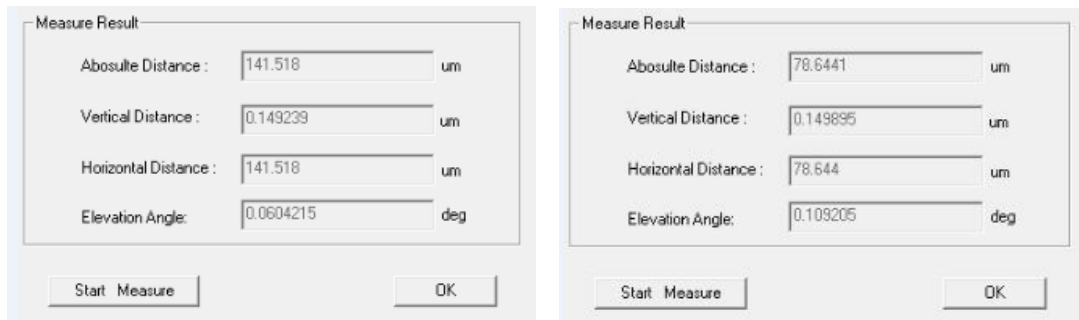
Width of the pixel



Mask design- 6



Simulation result in Fabsim



Length of the pixel

Width of the pixel

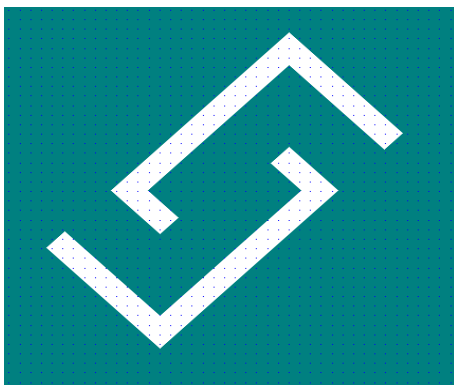
Fig.6.1: shows different designs with their corresponding Simulation results in Intellisuite FABSIm based physical simulator for above method.

6.1.2 Dry etching followed by Wet etching

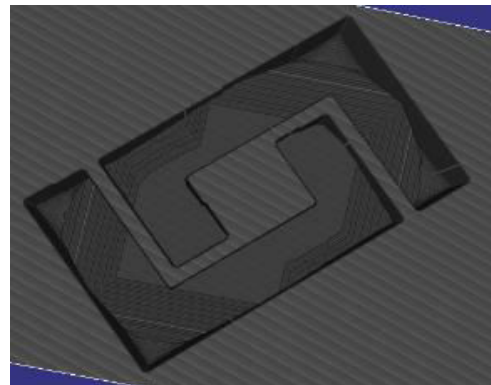
As in the previous chapter here in this method also we are going for dry etching initially and next wet etching but with different mask designs. In the subsequent sections we put simulation results for both the sub methods under the mentioned method for all the five mask designs.

6.1.2.1 DRIE followed by TMAH etching

Below fig.6.2 shows all the designs with their corresponding simulation results.



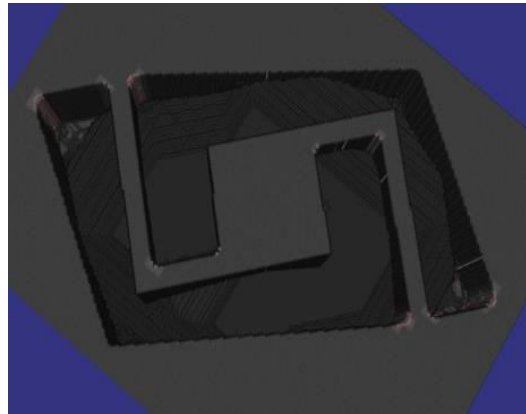
Mask design- 1



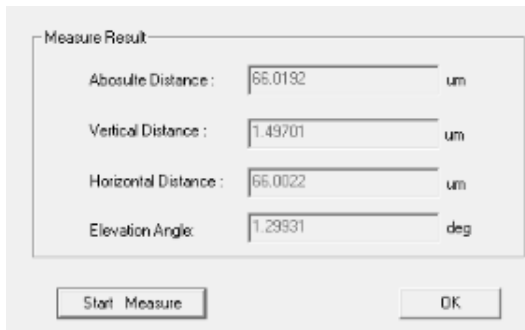
Simulation result in Fabsim



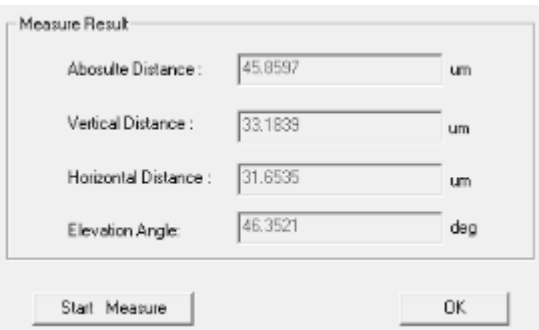
Mask design- 2



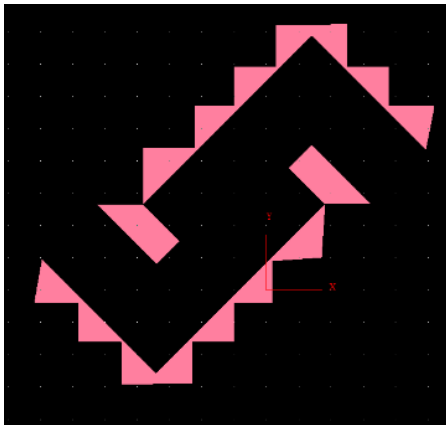
Simulation result in Fabsim



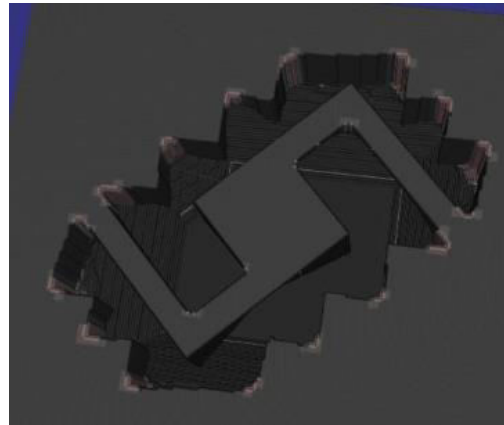
Length of the pixel



Width of the pixel



Mask design- 3



Simulation result in Fabsim

Measure Result

Absolute Distance : um

Vertical Distance : um

Horizontal Distance : um

Elevation Angle : deg

Length of the pixel



Mask design- 4

Measure Result

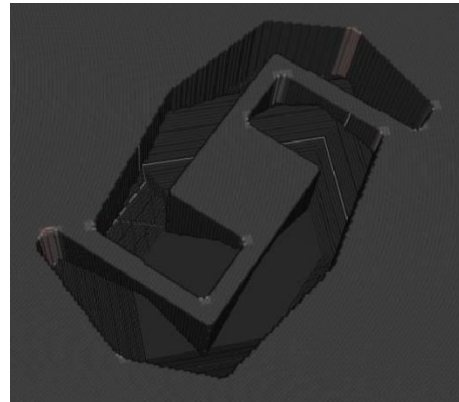
Absolute Distance : um

Vertical Distance : um

Horizontal Distance : um

Elevation Angle : deg

Width of the pixel



Simulation result in Fabsim

Measure Result

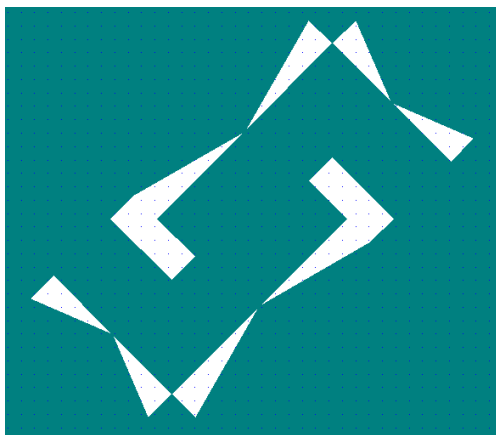
Absolute Distance : um

Vertical Distance : um

Horizontal Distance : um

Elevation Angle : deg

Length of the pixel



Mask design-5

Measure Result

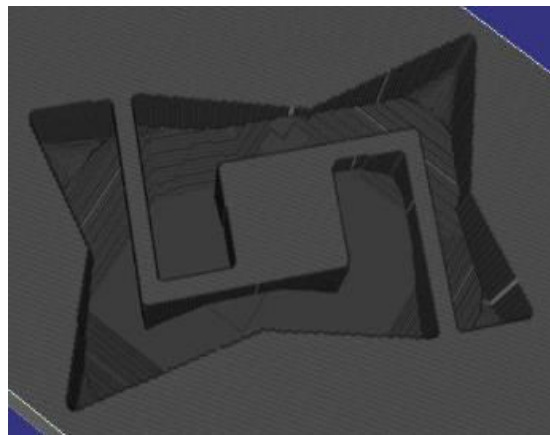
Absolute Distance : um

Vertical Distance : um

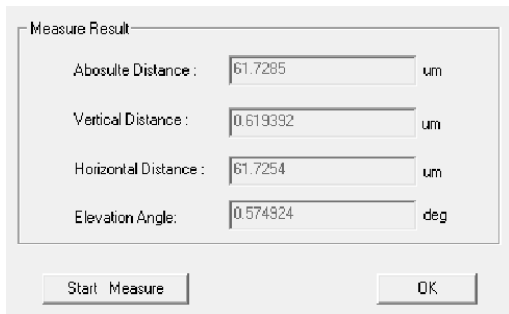
Horizontal Distance : um

Elevation Angle : deg

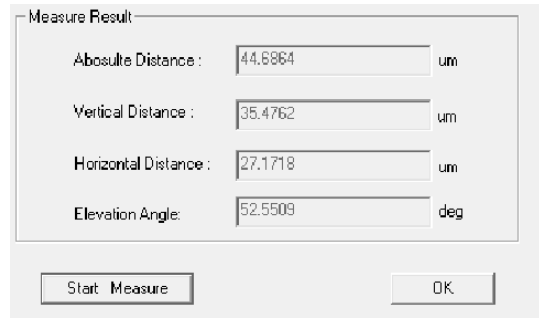
Width of the pixel



Simulation result in Fabsim



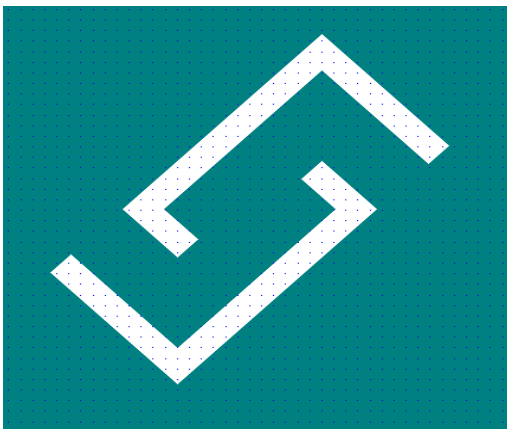
Length of the pixel



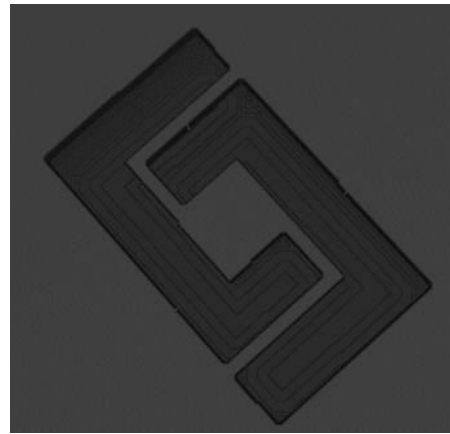
Width of the pixel

Fig.6.2: shows different designs with their corresponding Simulation results in Intellisuite FABsim based physical simulator for above method.

6.1.2.2 DRIE followed by HNA etching



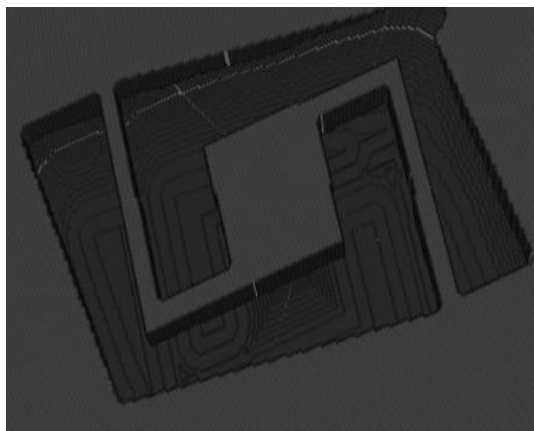
Mask design-1



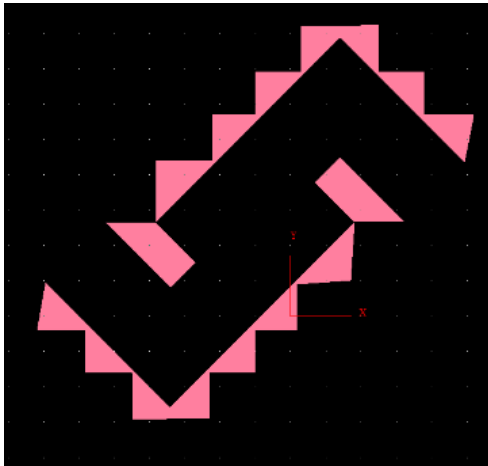
Simulation result in Fabsim



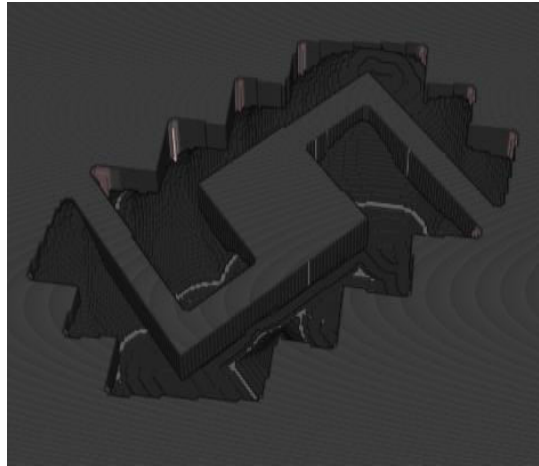
Mask design-2



Simulation result in Fabsim



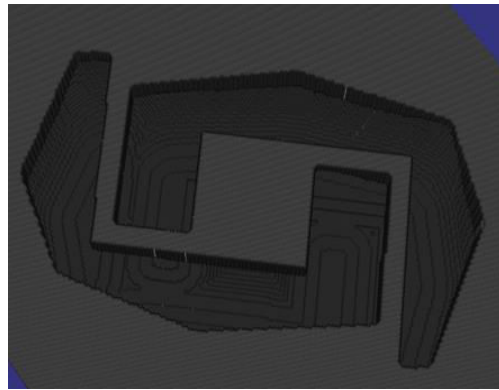
Mask design-3



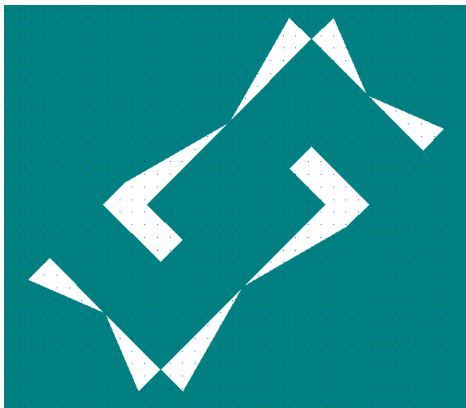
Simulation result in Fabsim



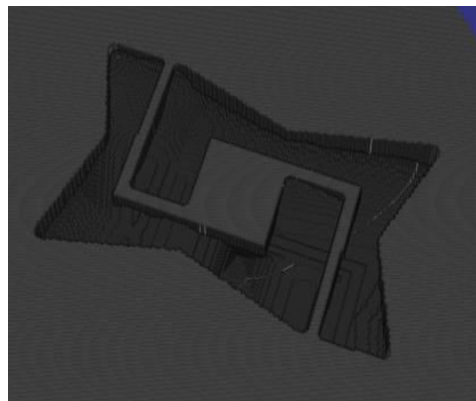
Mask design-4



Simulation result in Fabsim



Mask design-5



Simulation result in Fabsim

Fig.6.3: shows different designs with their corresponding Simulation results in Intellisuite FABSIm based physical simulator for above method.

In this case we have observed length and width calculated per pixel are same as that of the previous method i.e. DRIE followed by TMAH etching. Hence the table showing length and width of pixel is not explicitly put here. The area per each pixel is dependent on DRIE step which actually depends on the dimension of mask used in the 1st etching step. So in this method the area of each pixel of microbolometer sensor is almost equal to the area designed for mask in the 1st etching step.

CHAPTER 7

Fabrication results of Microbolometer

7.1 Microbolometer

The microbolometer is fabricated using the mask as shown in the previous chapter (fig.6.2). The fabrication process is followed as per the simulation results achieved in the Intellisuite Fabsim. The process followed for micro bridges and microbolometer is almost same except for one extra step in the fabrication of microbolometer. We will discuss the difference in the coming sections.

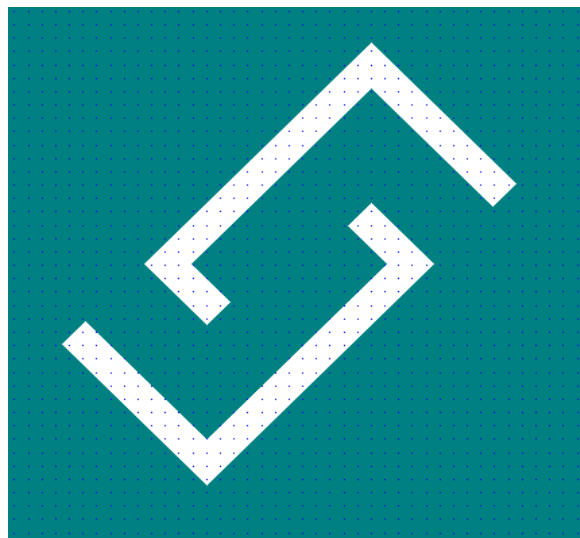


Fig.7.1 Shows the basic mask design for fabricating bolometer.

Figure 7.1 shows the mask used for the fabrication of bolometer. Using this mask the oxidized wafer was patterned and oxide was removed selectively in Hydrofluoric Acid (HF) and further the exposed silicon was etched in TMAH.

We have first started the fabrication procedure with a bright field mask suitable for a negative photo resist. Only the device area where we need to etch is blocked and the remaining mask is bright. We used AZ 5214 (image reversal) for this process. The results were not good with SU-8, so we moved to AZ 5214. Using AZ 5214 photo resist, we could achieve the proper etching and required profile after the first step. All the results were compared and are matched with the simulation results.

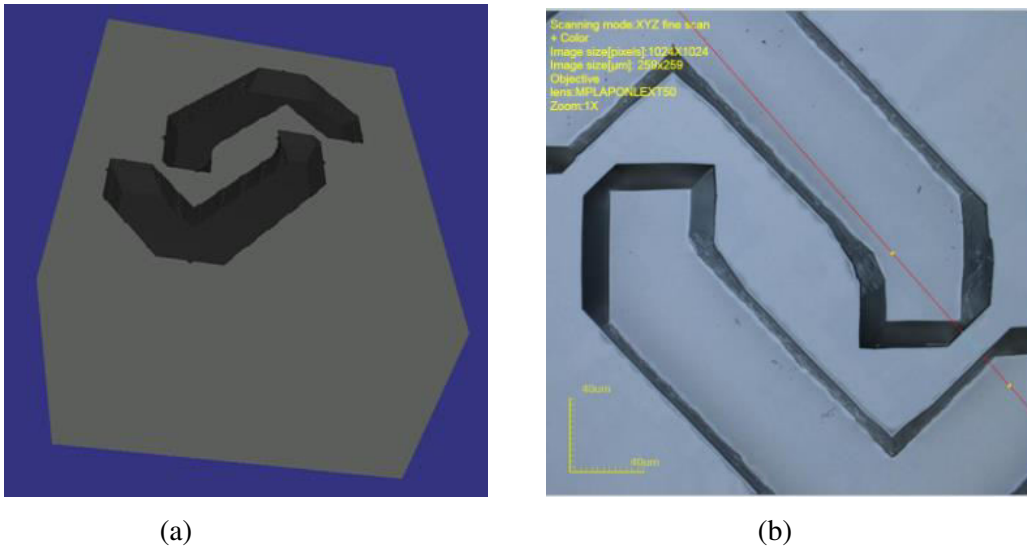


Fig7.2 (a) shows the simulation result of the bolometer (b) shows the confocal microscope image after the first step.

The first step etching was achieved properly and successfully. The etch profiles are shown in the fig.7.3 below. It shows both contour and the cut line of the etched portions. The etch depth achieved was 20 μm as shown in the figure.

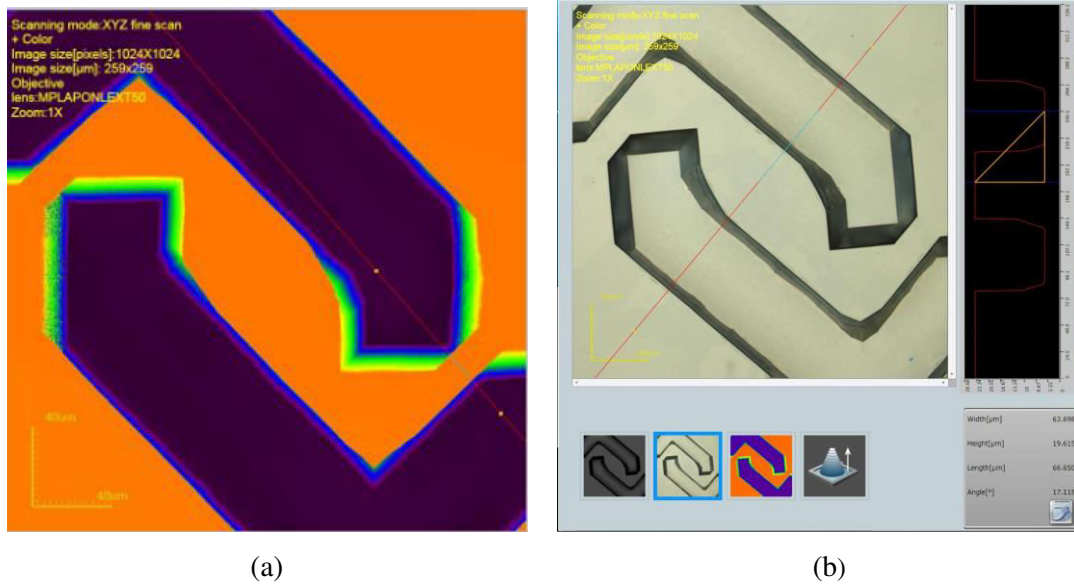


Fig 7.3 (a) shows contour plot of the etched bolometer after first step. (b) shows the profile of the etched silicon after the first step.

The first step lithography was done using low vacuum mode in the lithography system which will make the mask and wafer in contact. This will help us achieve the same dimensions of the mask on the wafer since the diffraction of light is minimised. But after the first step etching, when a trench of 20μm depth is formed, even if the low vacuum mode is used proper patterning can't be achieved using negative photoresist.

7.2 Issues faced in fabrication process

7.2.1 Issue with negative photo resist.

For transferring the design on to the oxidized silicon wafer, we use lithography in low vacuum mode (instead of proximity mode). In the first step etching, we etch for approximately 10μm. While processing lithography for the second step, even though we use lithography in low vacuum mode, the gap between the mask and the bottom surface where the design is to be patterned is 10 μm. But our feature size itself is 10μm. This will cause the light to diffract and expose the area, which actually have to be protected. This will cause the negative photoresist to form cross links and the photoresist will not be developed.

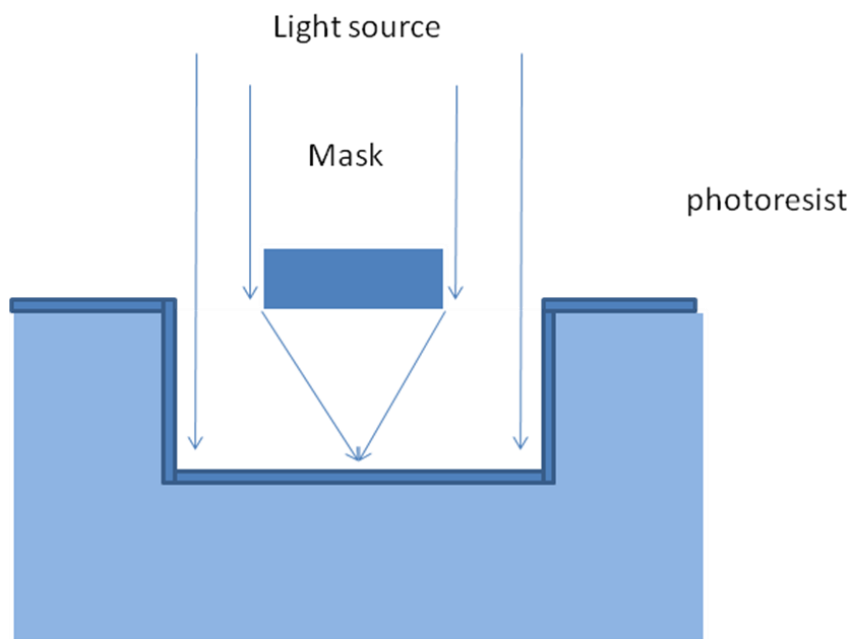


Fig.7.4 Shows the diffraction of light patterns when using negative photoresist and suitable mask

So to avoid this problem, we changed the mask to a dark field mask, where the entire mask is dark and the required pattern is transparent. This also has the chance of breaking the cross links at the sidewalls but the distance is more from line edge to the side wall. So the side wall will be protected.

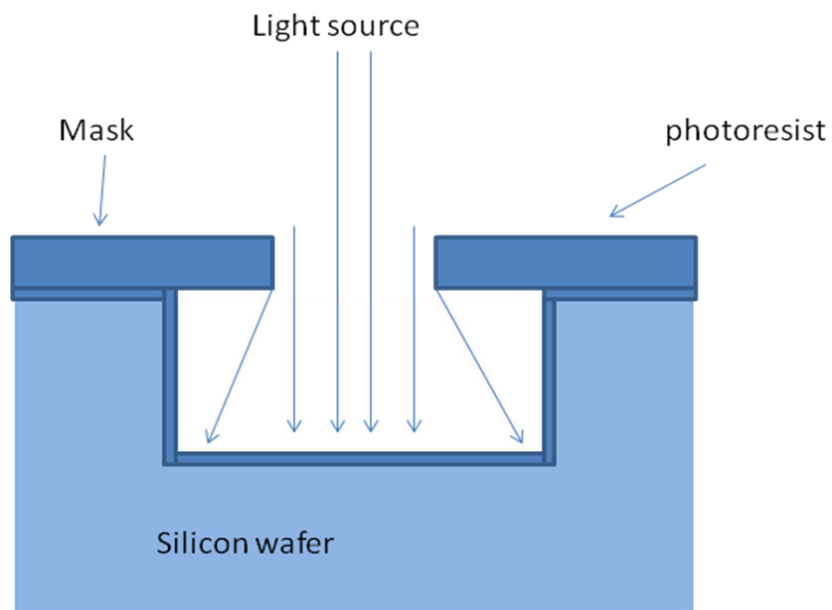


Fig.7.5 Shows the diffraction of light patterns when using negative photoresist and suitable mask

7.2.2 Side walls protection

Now using the dark field mask we have proceeded with the same process. When proceeded for the second step, the problem now aroused is that the side wall protection. When we spin the positive photo resist, the device should be protected from top and sideways. Due to the less viscosity and the uneven device structure, we could not protect the top surface of the structure

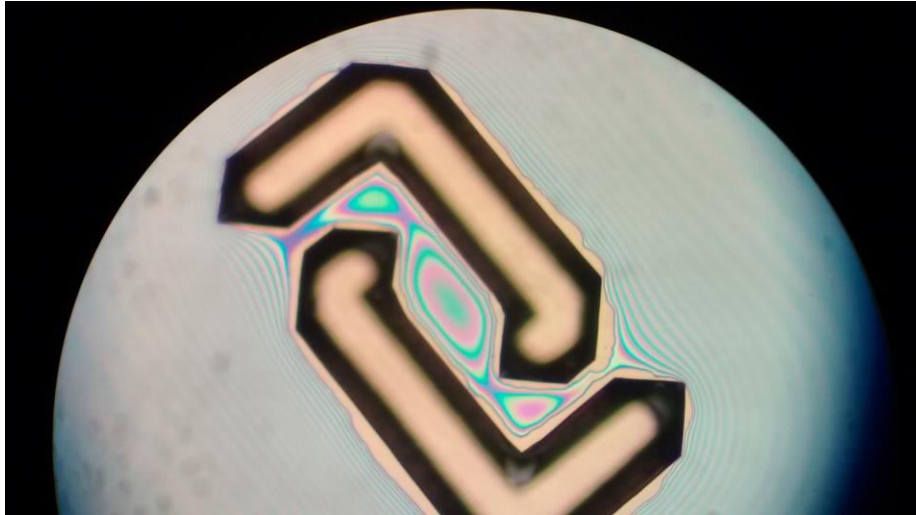


Fig.7.6 showing the spun photoresist not protecting the edges on the device.

To overcome this problem we tried out various methods

- Hanging oxide
- Using primer
- Using AZ thick photo resist
- SiN

Hanging Oxide

After the first step we usually remove the oxide and then oxidize it again. The problem with the positive photoresist is that it is not protecting the top surface only at the edges. Now if the hanging oxide that is left, without removing, that is achieved after the under etch that happened in the first step, then when the photo resist is spun, we still have a safe side of 10 μm . In this method, we could protect the top surface but the sidewalls were again unprotected.

Using Primer:

HMDS primer is used with positive photoresist for good adhesion. The silicon wafer is treated in vapor prime and then spin coat the positive photoresist. This method also did not give the required result.

SiN

This is one more option to overcome this problem. In this case, we initially deposit SiN on the silicon substrate. Now follow the same procedure for first step. Now we have a hanging SiN after the under etching of the silicon. Now we can oxidize the Silicon wafer. The sidewalls of the silicon are now protected by the oxide. Further we can spin coat the photoresist and just flood expose the Silicon substrate. This will expose the photoresist only at the opened areas between the hanging SiN. We need not use a mask also.

Thick Photoresist

Thick photo resist has high viscosity and forms a thick layer of photoresist when spun. A thickness of approx 12 μm is achieved using this thick photoresist. We used AZ4620 thick photoresist to overcome this issue. We exposed the sample for 100 sec at the lamp intensity of 4 as per the data sheet of the photoresist. The developer used is AZ400K. Diluted the developer in the ratio of 1:4 (developer:DI water).

Thus using the thick photoresist, the top surface and the sidewalls were protected properly. The litho was done and the required area was exposed in the trench. The oxide was removed and proceeded for further steps.

7.3 HNA etching

The difference in the fabrication of micro bridges and micro bolometers is an extra step of HNA etching. This results due to the structure and the shape of the mask design that we use here. In case of micro bridges it is only a one-dimension. In bolometer there are both concave and convex edges encountered during the etching process. The concept explained in the initial chapters about the 45° rotation is valid but with some restrictions. When we create an rectangular/square opening with edge at 45° to the wafer flat, the etch profile of the silicon will be perpendicular and not a 54.7° tilt. The etchant will not be able to see the 111 plane and so it etches perpendicularly. But this happens only at the middle of the line (edge). At the edges the etchant will face 111 plane and will not be able to etch perpendicularly. When such processed sampled, after creating a square pattern (aligned at 45° to wafer flat) etched for long time will create a square structure superscribing the initial square and with a pyramid structure. This is same as patterning a square parallel to the wafer flat.

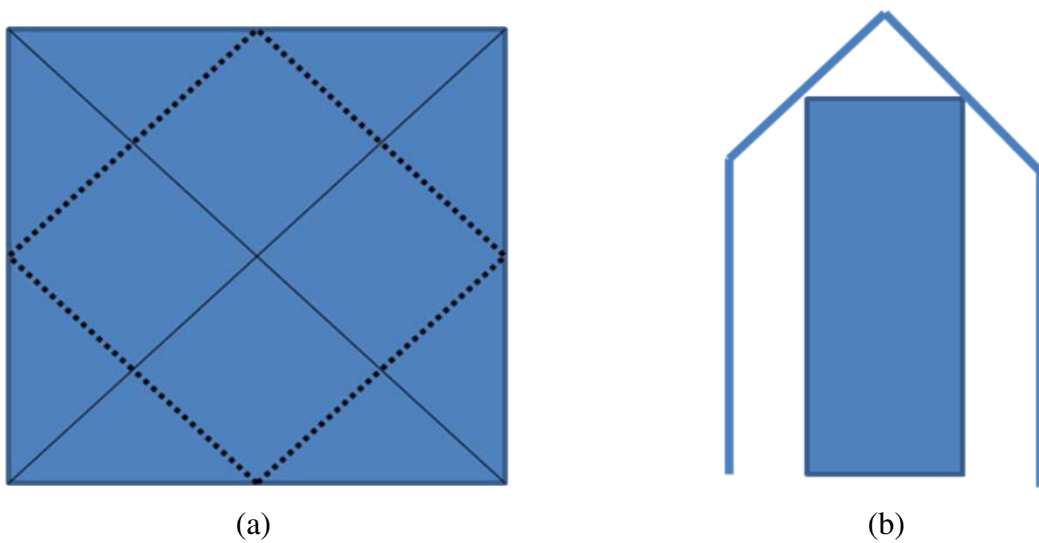


Fig.7.7 (a) Shows the etch profile of silicon when etched in TMAH with openings aligned 45° to the wafer flat. (b) etch profile observed in the bolometer structure.

This issue is seen while fabricating the bolometer at the concave edges. So to avoid this issue we go for HNA etching which is isotropic etchant and etches all the planes. This will remove the hurdle of 111 planes and clears the obstacle for the next TMAH etching.

One more reason for HNA etching is that, the TMAH etching will lead to a super scribing square when a square with 45° angle is etched for sufficiently long time. So at the concave edges while etching the bolometer structure, the same phenomenon is observed. When the same mask is used for the second time, the edges (as shown in the figure) get exposed and the top surface is not protected. So when the sample is put in TMAH for etching, it starts to etch from the top surface also which is not desirable.

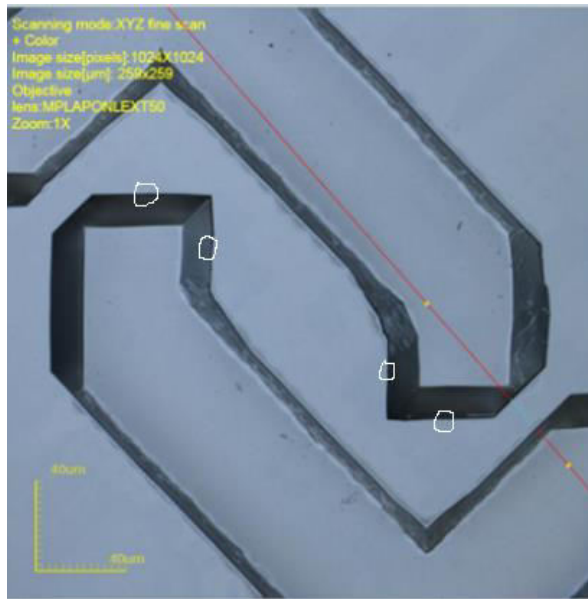
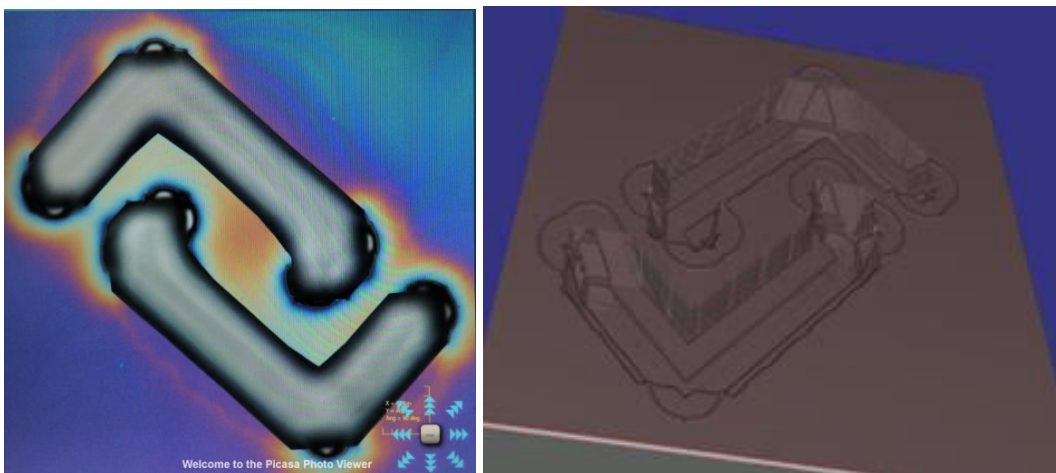


Fig.7.8 Shows the edges where the mask will expose the unwanted areas after first step

Once the lithography is over for the second step, HNA etching was done to break the (111) planes as explained previously. HNA etching is isotropic and etches in all directions. The profile of the etched silicon after HNA etching is shown in the fig 7.9. This will not only help in eliminating the 111 planes but also in realizing the proper shape of the bolometer sensor. The HNA etchant was prepared in the ratio of 11:7:4 as Acetic Acid:Nitric acid:HF



(a)

(b)

Fig.7.9 (a)Shows the fabrication result after the HNA etch. (b) simulation result after HNA etch.

Again the existing oxide is removed and oxidized the processed wafer for further steps. After oxidizing, again the photoresist is spun and patterned using lithography and oxide is etched selectively in the trenches and put in TMAH for further etching. This final step etching will release the hanging structure. All the etchings are calculated and done according to the data obtained from the simulations. The TMAH was used in the ratio of 2:3 TMAH : DI water. The silicon etching in TMAH was done at 75⁰C. The etch rate is approximately 0.8-1 $\mu\text{m}/\text{min}$ at 75⁰C. A proper careful and calculated etching is required to take care that the sensor membrane is neither over etched nor etched less.

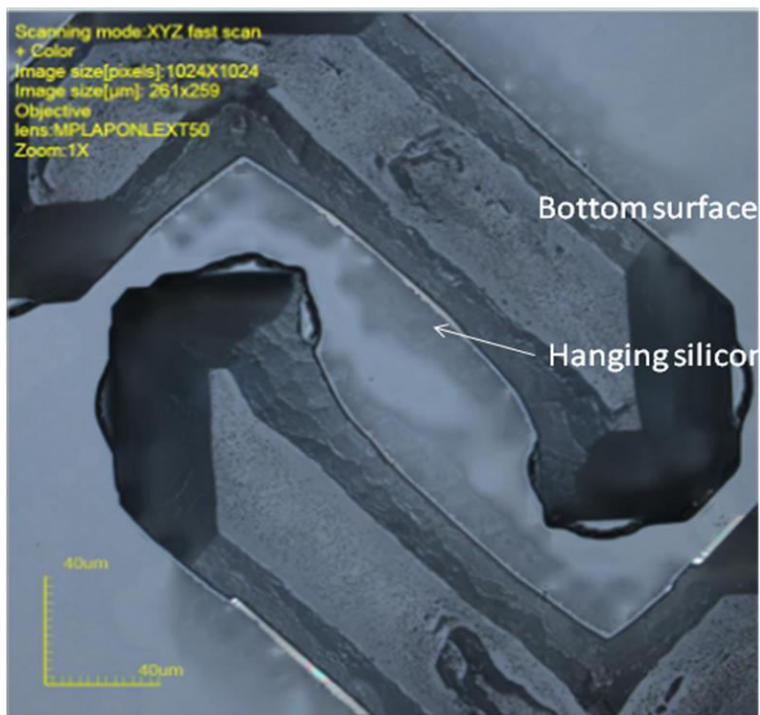


Fig.7.10 Shows the image of the fabricated microbolometer sensor after complete process.

SEM analysis was done for the sample. The SEM images after first step and final step are shown below. We can observe the slant profile in the bolometer after first step.

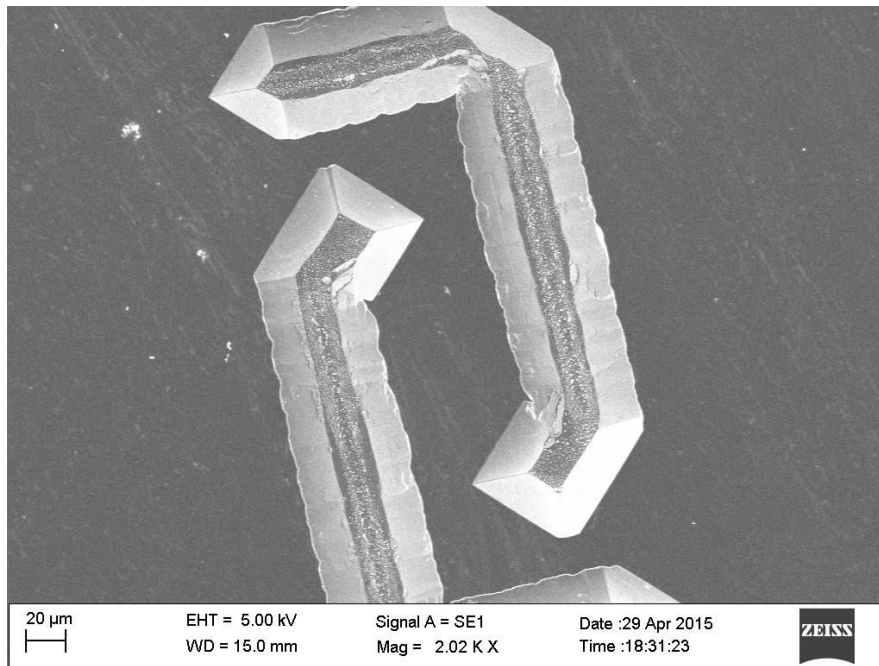
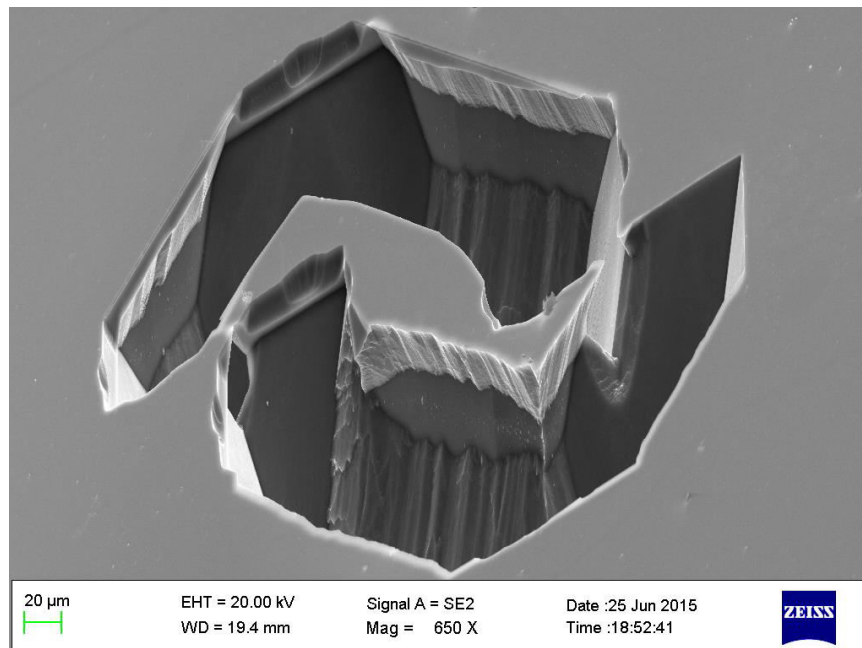
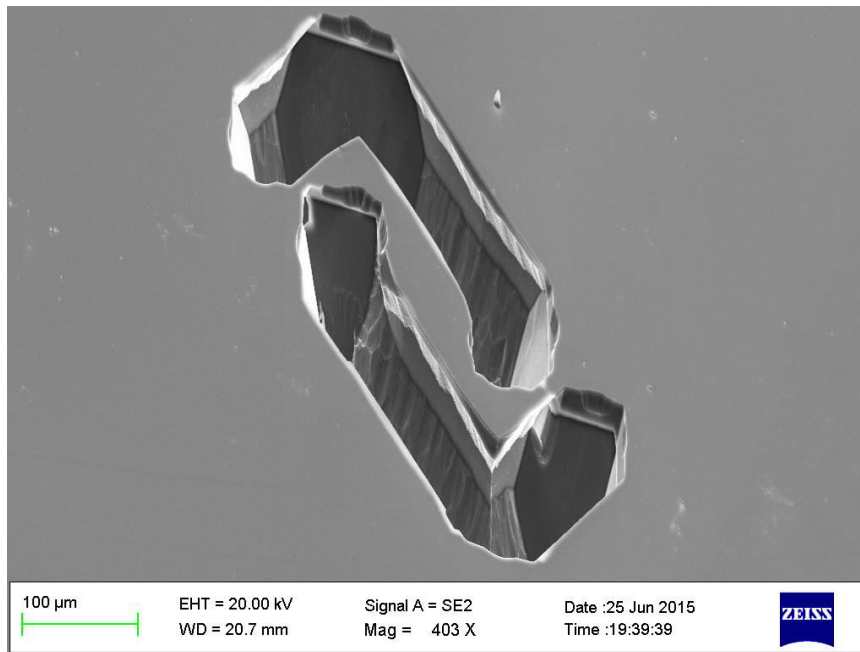


Fig.7.11 Shows the SEM image of the microbolometer after the completion of the first step.



(a)



(b)

Fig.7.12 (a)&(b) Shows the SEM images of the microbolometer after the complete process.

7.4 Fabrication of an array of bolometers

An array of such microbolometers are required to fabricate for the thermal imaging purpose. The fabrication of an array will still consume less area per pixel when considered the external area common for two adjacent pixels. A design for array was also done and processed the first step of the array. Figure.7.13 shows the first step fabrication result of the array.

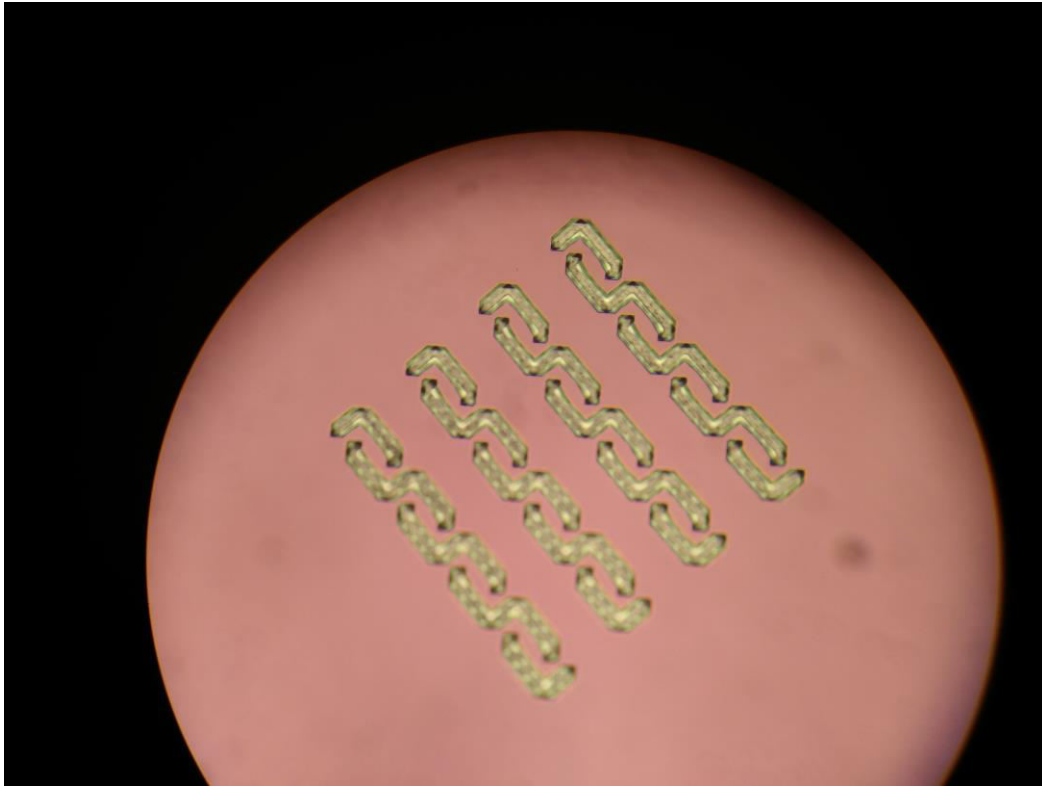


Fig.7.13 Shows the fabrication result of the array of bolometers after first step.

Chapter 8

Comparative case study of Making Microbolometer Sensor

8.1 Comparisons between only wet etching and dry followed by wet etching

- In the 1st method of fabricating the device we have used only one mask and isotropic and anisotropic wet etchants for making the detector which results in low cost method of fabricating the device.
- But the process is somewhat complicated being controlled by the time of etching and depth of etching and the second thing we have started with 128 μm X60 μm pixel of mask and should expect the device of same size but taking the advantage of horizontal etching results in the increase in pixel dimension, due to which the device consumed an area of 150 μm X80 μm . So we need to consume some significant amount area in fabricating microbolometer sensor in this method. So the pixel fill factor is not pretty good.
- In the 2nd method of fabricating the device which required two masks and DRIE makes the process more costly as compared to the previous process.
- But it gives certain advantages because the TMAH etching is required only in the 2nd etching step where the timing of etching and depth is not that stringent as that of 1st method where we have taken care of time of etching and etch depths in all of the three etching steps and optimized that. Secondly if we target for the dimension of device i.e. 128 μm X60 μm then we will be having pixel area of that much only as the important step is the 1st etching step in terms of area consumed per pixel taken care by DRIE hence not allowing any other direction of etching except in vertical.

Table-8.1 shows the calculation and comparisons of area calculated of all the methods of fabricating microbolometers for all the designs.

Table-8.1 showing area calculate for microbolometer fabrication using all the designs

	Area per pixel using Method1(μm^2)	Area per pixel using Method2-sub method-1(μm^2)	Area per pixel using Method2-sub method-2(μm^2)
Design1	12095	2800	2800
Design2	10290	2090	2090
Design3	10080	2515	2515
Design4	9105	2574	2574
Design5	11130	1684	1684

8.2 Comparisons between sub methods under method-2

Comparing the two processes under dry followed by wet etching, we observed using HNA in 2nd step of etching consumes more area inside the bulk Si as compared of using TMAH in 2nd step. Below fig.8.1 shows the simulated result showing the maximum distance etched by both the processes. Where it is easily visible HNA is consuming more area as compared of using TMAH for the same mask.

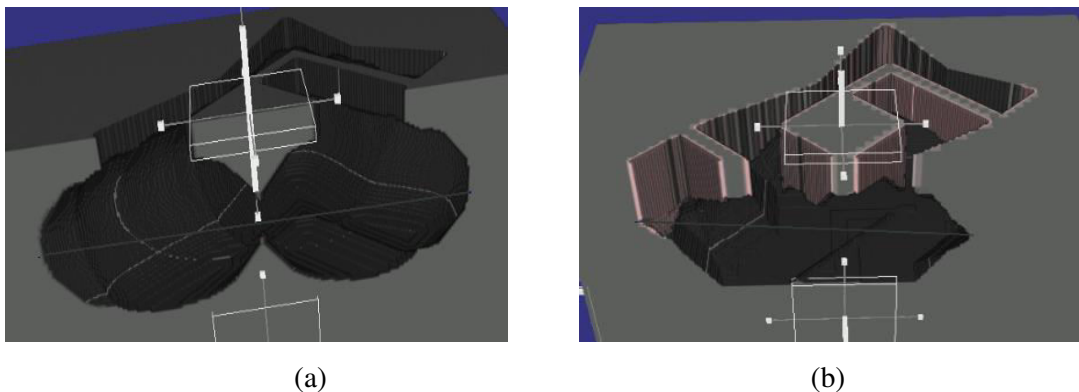


Fig.8.1: (a) shows under etch inside bulk Si using HNA and (b) shows under etch inside bulk Si using TMAH.

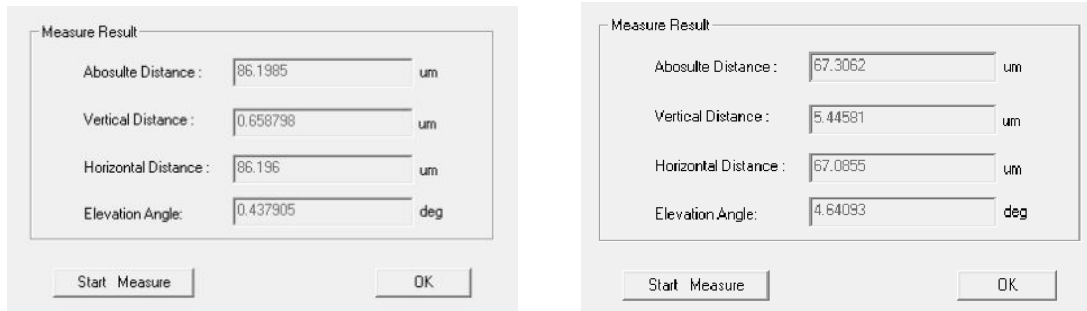


Fig.8.2: (a) shows the table calculating maximum distance etched under bulk Si using HNA and (b) shows maximum distance etched inside bulk Si using TMAH.

8.3 Comparisons between proposed methods and existing methods of making microbolometer sensor

Table below shows comparisons between the existing methods of fabricating microbolometer and proposed methods.

Table-8.1 shows comparison between existing method and proposed method to fabricate microbolometer sensor.

METHODS	COST	RELIABILITY	EASE	SENSING
CMOS line	LOW	HIGH	MODERATE	MODERATE
HETEROGENEOUS 3D INT.	HIGH	LOW DUE TO HANGING STRUC TURE	DIFFICULT	High
PRESENT METHODS	LOW-method-1 Moderate Method-2	HIGH as Si is the part of the substrate In both methods	MODERATE	MODERATE if used in CMOS line high if in heterogeneous 3D with VO _x

Chapter 9

Conclusion and Future Work

9.1 Conclusion

In the present work we have proposed cost effective and novel way to make microbolometer sensor as well as Si microbridges. Where the proposed method of making Si Micro bridges or cantilever beams is based on simple wet etching technique i.e. the frontend bulk micromachining which reduces the requirement of clean room and hence the cost associated with it. The efficient mask designs proposed decreases foot print of individual pixels hence increases overall efficiency of the device which may be simple Si micro bridge or cantilever or any of the complicated structure or may be array of any of the above.

The methods proposed in the work to fabricate microbolometer sensor are simple and majorly consists of etching steps only. These methods doesn't require any diffusion or electrochemical etch stopping technique, which may complicate the process, rather the simple wet etching steps avoids the requirement of clean room which can reduce the cost of making the device specially the method 1 way of fabricating microbolometer sensor.

9.2 Future Scope of Work.

The present work was focused to make microbolometer sensor in a simple and cost effective way. The scope for the future work is listed below.

- Optimization and characterization of the microbolometer sensor.
- Deposition of high TCR microbolometer sensing material e.g. VO_x to increase sensitivity of the device.
- Mirror material deposition at bottom of the sensor for capturing more IR radiations.
- Implementation of an array of bolometers.
- 3D integration of microbolometer sensor with its corresponding ROIC.

References

- [1] *Darius Jakonis , Christer Svensson , Christer Jansson* “Readout architectures for uncooled IR detector arrays” *Sensors and Actuators* 84 _2000. 220–229.
- [2] *Gregory T. A. Kovacs, Member, IEEE, Nadim I. Maluf, Member, IEEE, and Kurt E. Petersen, Fellow, IEEE* “Bulk Micromachining of Silicon” *Proceedings of the IEEE*, VOL. 86, NO. 8, AUGUST 1998.
- [3] *Frank Niklaus, Christian Vieider, Henrik Jakobsen* “MEMS-Based Uncooled Infrared Bolometer Arrays – A Review” *MEMS/MOEMS Technologies and Applications III*, III, edited by Jung-Chih Chiao, Xuyuan Chen, Zhaoying Zhou, Xinxin Li, *Proc. of SPIE Vol. 6836, 68360D*, (2007).
- [4] *Selim Eminoglu, Deniz Sabuncuoglu Tezcan, M. Yusuf Tanrikulu, Tayfun Akin* “Low-cost uncooled infrared detectors in CMOS process” *Department of Electrical and Electronics Engineering, Middle East Technical University, Ankara 06531, Turkey. Sensors and Actuators A* 109 (2003) 102–113.
- [5] *Deniz Sabuncuoglu Tezcan**, *Selim Eminoglu*”, *Orhan Sevket Akar***, and *Tayfun Akin**,* *Department of Electrical and Electronics Engineering, Middle East Technical University, Ankara, Turkey* “A Low Cost Uncooled Infrared Microbolometer Focal Plane Array Using The Cmos N-Well Layer” ** *TUBITAK-BILTEN*, Middle East Technical University, Ankara, Turkey.
- [6] *Ben Kloeck, Scott D. Collins, Nico F. De Rooij, And Rosemary L. Smith* “Study of Electrochemical Etch-Stop for High-Precision Thickness Control of Silicon Membranes”, *IEEE TRANSACTIONS ON ELECTRON DEVICES*. VOL. 36. NO. 4. APRIL 1989.
- [7] *Frank Niklaus, Adit Decharat, Fredrik Forsberg , Niclas Roxhed , Martin Lapisa, Michael Populin ,Fabian Zimmer, Jörn Lemmb, Göran Stemme* “Wafer bonding with nano-imprint resists as sacrificial adhesive for fabrication of silicon-on-integrated-circuit (SOIC) wafers in 3D integration of MEMS and ICs” *Sensors and Actuators A* 154 (2009) 180–186.
- [8] *Ben Kloeck, Scott D. Collins, Nico F. De Rooij, And Rosemary L. Smith* “Study of Electrochemical Etch-Stop for High-Precision Thickness Control of Silicon Membranes” *IEEE TRANSACTIONS ON ELECTRON DEVICES*. VOL. 36. NO. 4. APRIL 1989.
- [9] *Ei-no H. Klaassen **, *Richard J. Reay, Christopher Storment, Gregory T.A. Kovacs* *Center for Integrated Systems. CIS-X 202. Stanford University. Stanford, CA 94305-4075 USA* “Micromachined thermally isolated circuits” *Sensors and Actuators A* 58 (1997) 43-50.

- [10] *M.C. Acero, J. Esteve, Chr.Burrer, A. Gotz* “Electrochemical etch-stop characteristics of TMAH:IPA solutions “ Sensors and actuators A46-47(1995) 22-26.
- [11] *Ernest Bassous* “Fabrication of novel Three- Dimensional microstructures by anisotropic etching of (100) and (110) Silicon” IEEE Transactions on Electron Devices, Vol. ED-25, NO.10 October 1978.
- [12] E.chen Applied physics 298r.
- [13] *Weileun Fang* “Design of bulk micromachined suspensions” J. Micromech. Microeng. **8** (1998) 263–271.